Geoderma 295 (2017) 53–68

Contents lists available at ScienceDirect

Geoderma

journal homepage: www.elsevier.com/locate/geoderma

Geochemistry of a soil *catena* developed from loess deposits in a semiarid environment, Sierra Chica de Córdoba, central Argentina

Andrea I. Pasquini [a,b,*], Verena A. Campodonico [a], Sabrina Rouzaut [a,b], Viviana Giampaoli [c]

[a] Centro de Investigaciones en Ciencias de la Tierra (CICTERRA). Consejo Nacional de Investigaciones Científicas y Técnicas (CONICET) y Universidad Nacional de Córdoba. Av. Vélez Sarsfield 1611, X5016CGA Córdoba, Argentina
[b] Facultad de Ciencias Exactas, Físicas y Naturales, Universidad Nacional de Córdoba. Av. Vélez Sarsfield 1611, X5016CGA Córdoba, Argentina
[c] Departamento de Estatística, Instituto de Matemática e Estatística, Universidade de São Paulo. Rua do Matão, 1010, CEP 05508-090 São Paulo, Brazil

ARTICLE INFO

Article history:
Received 29 May 2016
Received in revised form 5 December 2016
Accepted 26 January 2017
Available online xxxx

Keywords:
Pedogenic processes
Mollisols
Weathering
Rare earth elements
Quaternary

ABSTRACT

A catenary sequence of soils formed on reworked loess under semiarid climatic conditions was studied. Four soil profiles located on the piedmont of Sierra Chica de Córdoba, central Argentina, were described, classified and geochemically analyzed. All soils, developed on summit, shoulder, backslope, and toeslope positions, were classified as Mollisols. Decarbonatation-carbonatation, melanization, and argilluviation are the main pedogenic processes recognized in these soils, which appear to control the differentiation of genetic horizons along the *catena*. Different geochemical approaches indicate that there are not substantial variations in the chemical composition of the studied soils along the *catena*, with the exception of the soil in the toeslope position, which exhibits slightly differences. In general, all profiles show weak depletions of mobile elements (Ca, Na, Mg, Sr, U) in the upper continental crust UCC-normalized diagrams which are attributed to a slight chemical alteration. Other elements, such as Fe, Cr, Co and Ni, also exhibit depletions compared to UCC, which can be explained by the alteration of ferromagnesian silicates, but can also be an inherited feature from the parent material. The significant enrichment in As compared to UCC, evident in all profiles along the *catena*, is also a typical feature of the pampean plains' loess of Argentina. So, the chemical differences in the profile located on the toeslope are mainly attributed to the supply of materials from local sources, i.e., crystalline basement and sedimentary rocks, due to its position in the *catena*. Statistical correlations and multivariate cluster analyses reinforce the assumption that the geochemistry of the studied soils is inherited from the parent material. In addition, chemical indices (CIA, ICV), elemental ratios (Ba/Sr, Rb/Sr) and the A-CN-K ternary diagram indicate an incipient degree of chemical alteration for these soils, compatible with the weathering regime prevailing in the region. Thus, the differentiation of genetic horizons along the *catena* is the result of weak weathering and pedogenic processes, which have not been strong enough to mask the chemical imprint of the parent material.

1. Introduction

Geochemical cycles of elements are determined by natural processes and, eventually, are also affected by human activities. In the exogenous cycle, weathering and pedogenesis play an important role in releasing and mobilizing the constituents of rocks, sediments, and/or soil parent materials. Samouëlian and Cornu (2008), in a remarkable conceptual review, pointed out that the traditional models of soil formation and evolution are based on the organization and distribution of solid phases. The latest models, however, incorporate the concept of "pedogenic processes", which involve physical, chemical and biological transformations. All these processes that occur at the interface between the parent material, the biosphere and hydrosphere, i.e., the pedosphere, determine the mobilization and redistribution of chemical elements in a soil profile.

Soil science has traditionally explored the variability of several physicochemical properties and the mineralogical composition of soils in the profile; however, there are few works that deal with the dynamics of chemical elements mobility, and particularly those regarding trace elements behavior. In this sense, some recent examples can be mentioned. Laveuf and Cornu (2009) have conducted a thorough analysis of the dynamics and mobility of rare earth elements in order to quantify the contribution of the different pedogenic processes on the distribution of these chemical elements in a soil profile. Other recent studies which analyze the distribution of chemical elements in response to pedogenic processes and weathering are those of Bini et al. (2011), Caspari et al. (2006), Chittamart et al. (2010), Levitan et al. (2015), Prakongkep

* Corresponding author at: CICTERRA. Av. Vélez Sarsfield 1611, X5016CGA Córdoba, Argentina.
E-mail address: apasquini@unc.edu.ar (A.I. Pasquini).

http://dx.doi.org/10.1016/j.geoderma.2017.01.033
0016-7061/

et al. (2008), Prudêncio et al. (2010), Thanachit et al. (2006), to mention a few. These authors pointed out that trace elements analysis in pedological studies are useful to detect anomalous distributions of elements in soils, to identify elements associated with mineral deposits, to analyze how the geochemical soil data reflects the underlying geology and how far the differences can be attributed to weathering, sediment transport and/or pedogenesis. All this information could be, in turn, valuable to land and natural resources managing.

In this work we describe, classify and characterize, from a geochemical point of view, a catenary soil sequence derived from loessic parent material developed on the eastern foothills of the Sierra Chica de Córdoba in central Argentina. A *catena* can be defined as a soil transect, from the top to the base of a slope, usually interpreted as a perpendicular transect to the contour of the slope (Schaetzl, 2013). This author also noted that while the relief, as a soil formation factor, is passive, its function is to provide potential and kinetic energy to the system, through its influence on the flow of matter and energy in the soil-landscape system. The *catena* concept is then used to refer to soils developed along a slope, but formed thereon parent material, so that, all forming factors except the topography, are constant.

The parent material of the soils studied here is part of the largest loess deposit that extends along the southern plains of South America. The sediments that cover the Pampean Plain in Argentina have been first defined as loess by Heusser and Claraz (1866). Several works were conducted latter, during the first decades of the twentieth century (e.g., Döering, 1907; Frenguelli, 1918), but it was Teruggi (1957) who established the fundamental basis for further studies of the loess in Argentina. These latter researches include those of Iriondo (1997), Sayago (1995), Sayago et al. (2001), and Zárate (2003) among others, most of them focused on the origin, provenance and distribution of these wind-blown deposits.

The loessic sediments that constitute the parent material of the soils studied in this work have been described by Santa Cruz (1972) as General Paz Formation, later named Toro Muerto Formation by Candiani et al. (2001). According to Argüello et al. (2012), this material can be defined as *reworked loess* in the sense of Pye and Sherwin (1999), as the loess has been locally transported and redeposited by colluvial or fluvial processes, maintaining most of the characteristics of wind-blown deposits. Then, from now on, the term loess is used to refer to this reworked loess which constitutes the parental material of the studied soils. References regarding the geochemistry of loess in the Argentina's pampean region are not abundant in the literature. Gallet et al. (1998) have reported some geochemical data of pampean loess in Buenos Aires Province, as well as Buffa and Ratto (2009), Nicolli et al. (2010), and Smedley et al. (2002), who have also analyzed the geochemical composition of loess in the pampean region. Specifically in Córdoba Province, some works related to loessic soils are those of Argüello and Sanabria (2003) and Sacchi and Pasquini (1999). However, none of these studies included data of soil geochemistry.

Considering that it is assumed that the genetic and morphologic differences in a catenary soil sequence is mainly due to the influence of landscape position, the aim of this paper is to elucidate if significant differences are also discernible through the geochemistry in a soil *catena* developed in a semiarid environment. The particular objectives are: a) to describe and classify four catenary soils developed from the same parent material, b) to determine the geochemical composition of the soil profiles, c) to examine the behavior of major and trace elements in the catenary sequence, d) to analyze, by means of geochemical and statistical tools, the imprint of weathering and pedogenesis along the *catena*. In addition, we also provide geochemical data of loess deposits in central Argentina.

2. Materials and methods

2.1. Study area

The studied soils are developed along a west facing slope *catena* located in the eastern piedmont of Sierra Chica de Córdoba, Argentina (30° 58′S, 64° 09′W, Fig. 1), which represent the easternmost outcrops of the Sierras Pampeanas de Córdoba, in central Argentina. Geologically, the Sierra Chica region is characterized by a Precambrian plutonic-metamorphic basement (900–1000 Ma, Kraemer et al., 1993), mainly composed of schists and medium- to amphibolite-grade biotite tonalitic gneisses. Although less widespread, granitoids, marbles, and amphibolites are also recognized (Gordillo and Lencinas, 1979). The basement rocks are discordantly overlain by Mesozoic and Cenozoic sedimentary rocks. This sedimentary sequence was described by Santa Cruz (1972) and it is composed of continental polymictic conglomerates (Saldán Formation, Lower Cretaceous?), fluvial conglomerates and fluvial sands (Estancia Belgrano Formation, Lower Pleistocene?). Reworked loess sediments with disseminated calcium carbonate (General Paz Formation, Upper Pleistocene?) overlie in discordance these continental deposits, and the sequence culminates with fluvial and alluvial sediments named Río La Granja Formation (Holocene?).

The General Paz Formation is widely distributed along central Córdoba province. This wind-blown sediment is mainly composed of medium to fine silt and, to a lesser extent, of clay-size (~20%) and sand-size (~10%) fractions. It is massive, homogeneous, friable and pale yellow or buff. The mineralogical composition is mainly represented by volcanic glass, quartz, plagioclase and minor amounts of K-feldspar and calcite. Accessory minerals such as biotite, muscovite, and garnet, opaque phases, epidote, apatite, zircon, lamprobolite and pyroxenes, can also be recognized. The clay-size fraction is composed of illite (~89%), with scarce montmorillonite (~8%) and kaolinite (~2%) (Santa Cruz, 1978). The General Paz Formation overlies conglomerates interbedded with fluvial sands corresponding to Estancia Belgrano Formation, which constitutes, from a geomorphological point of view, the first level of the piedmont. The phenoclasts of these conglomerates mainly consist of granitic, pegmatitic and migmatitic rocks (~60–70%), with small proportions of amphibolites, schists and marbles. The most abundant minerals, in decreasing order of abundance, are quartz, plagioclase and K-feldspar.

The study area lies in Argentina's temperate zone, which is characterized by active atmospheric dynamics and the action of polar and subpolar fronts. The climate in the region is typically continental, semihumid to semiarid. Mean annual temperature ranges between 14 and 17 °C, and the irregular distribution of annual precipitation is a typical feature. About 80% of annual rainfall occurs during the austral summer due to humid air coming in from the north (Pasquini et al., 2006). Mean annual precipitation for the record period 1960–2015 is 815 mm, which is concentrated between November and April, i.e., the wet season (660 mm for the same record period).

Because of its geographical location, geological features, and climate, the region is characterized by an erosional regime defined as "weathering-limited" in the sense of Carson and Kirkby (1972), as it was already pointed out by Campodonico et al. (2014) and references therein. Weathering-limited scenarios are those in which the transport of material is more rapid than weathering, whereas in a "transport-limited" regime weathering rates exceed the transport rates (e.g., Stallard and Edmond, 1983). As a result, in a weathering-limited erosional regime, a significant part of the regolith is rapidly removed by physical processes and soil development is incipient.

2.2. Soil sampling and analytical determinations

Four soil profiles (Fig. 1) along a *catena* were described and sampled by genetic horizon according to Schoeneberger et al. (2002) and classified following the Soil Taxonomy (Soil Survey Staff, 2014). The *catena*

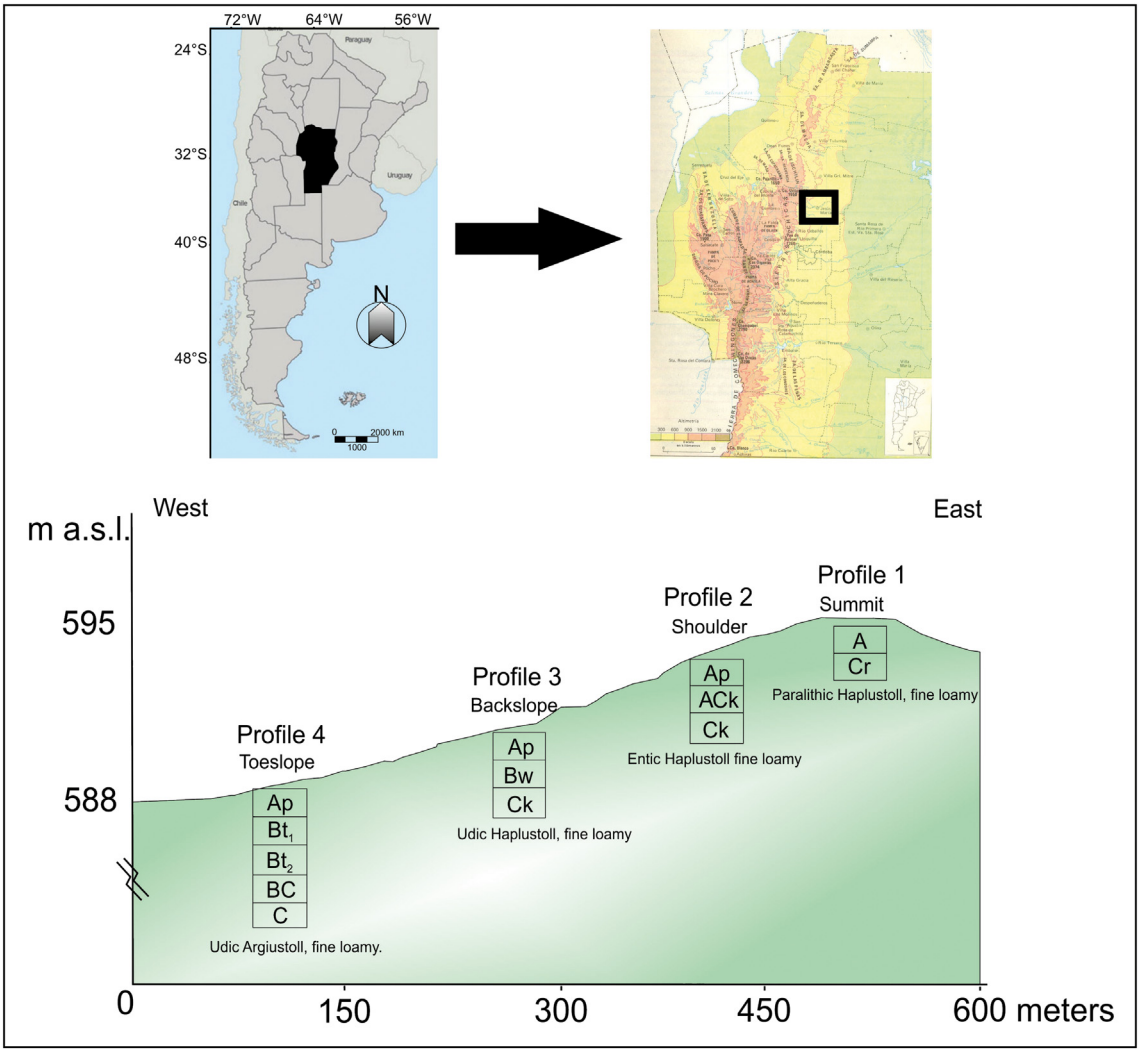

Fig. 1. Geographical location of the studied soils on the piedmont of Sierra Chica de Córdoba, central Argentina, and schematic representation of the *catena*.

has 600 m length and an average slope of 2%. The soils are located on summit (profile 1), shoulder (profile 2), backslope (profile 3) and toeslope (profile 4) positions (Fig.1). Standard determinations were carried out in situ, and approximately 2 kg of sample were taken of each identified horizon.

All soil samples of the four profiles were analyzed in laboratory, with the exception of Cr-horizon of profile 1 due to the presence of a paralithic contact. Soil samples were air-dried, crushed and passed through a 2 mm sieve to remove pebbles. Physico-chemical determinations were performed at the Ministerio de Agua y Energía de la Provincia de Córdoba, Argentina. Organic matter and carbonates were removed prior to particle size determination, using hydrogen peroxide and acetic acid respectively. The particle size distribution was determined by the pipette method (Schlichting et al., 1995) and wet sieving. Soil pH was measured in a 1:2.5 soil:water mixture by potentiometric methods. Organic carbon (OC) was determined by means of the Walkley-Black titration method (Walkey and Black, 1934) and total nitrogen by the Kjeldahl method (Bremner and Mulvaney, 1982). The exchangeable cations Ca^{2+} and Mg^{2+} were determined by complexometric titration, whereas K^{+} and Na^{+} were measured by flame photometry. The cation exchange capacity (CEC) was obtained by means of the ammonium saturation method at pH 7. Base saturation is informed as percentage (%BS), which is the proportion of the CEC occupied by the basic cations (i.e., Ca^{2+}, Mg^{2+}, Na^{+}, K^{+}); thus, if all the exchangeable bases total 100%, then there is no exchangeable acidity. In laboratory it was determined by the NH_4OAc method.

Major oxides and trace elements, including rare earth elements, were determined in a subsample free of organic matter and carbonates, in the bulk sample and in the <62.5 μm size-fraction at ACME Labs (Vancouver, Canada). The major chemical composition was measured by ICP-OES, whereas trace elements were determined by ICP-MS. Three blanks and five reference materials were analyzed. Duplicates were run every six samples in order to check the reproducibility of results.

2.3. Statistical tools

A linear regression model was used to explain the statistical relationship of the REE fractionation in the bulk samples and the <62.5 μm size-fraction. Since La_N/Yb_N is directly related to La_N, a regression model without intercept was employed. To elucidate the relationship between La_N and Yb_N, data of bulk samples and fine fractions were adjusted to models GAMLSS (Generalized Additive Models for Location, Scale and Shape, Rigby and Stasinopoulos, 2005). These models have the advantage of considering different type of probability distribution for the dependent variable and the final model can be selected by the generalized Akaike information criterion. Thus, it was determined that the Yb_N values follow a Weibull probability distribution considering the third parameterization (WEI3). The general expression for the mean model is: Mean (Yb) = $\exp(\beta_0 + \beta_1 La_N + \beta_2 \text{Group} + \beta_3 La_N * \text{Group})$,

where Group is the indicator variable group (i.e., bulk samples and fine fractions) and La_N * Group represents the interaction between La_N and the group.

To test the statistical association between major and selected trace element concentrations in the bulk samples of the studied soils, the Spearman's rank correlation coefficient was used. Chemical variables were standardized to avoid scale effects resulting from differences in magnitudes and measurement units. On the other hand, to reveal the association or groups of chemical elements and soil horizons, multivariate cluster analyses were employed. The agglomerative hierarchical clustering method of dissimilarity matrix, obtained from the standardized variables considering the Euclidean distance, was used. The optimal number of groups was obtained using the silhouette criterion. This is a method usually employed to evaluate the cohesion of individuals within a cluster compared to other groups. The observations with higher silhouettes values are best clustered.

3. Results and discussion

3.1. Soil properties and processes

Field appearance of soil profiles is shown in Fig. 2, and the morphological and physico-chemical properties of the genetic horizons are summarized in Table 1.

All soils have base saturation > 50%, pHs are circumneutral and the organic matter content of the A-horizons is >2%. According to these characteristics the soils have been classified as Mollisols, with different degrees of development depending on their position in the *catena*. The water table is deep and it does not affect the drainage of the soil profiles. The moisture regime of these soils is defined as ustic with transition to udic (Soil Survey Staff, 2014). The land uses in the study area are mainly corn and soy cultivation.

Profile 1 (on the summit position) has an A-horizon of 20 cm with few calcium carbonate concretions (Fig. 2). This topsoil is directly supported by the moderately cemented conglomerates of the Estancia Belgrano Formation in a paralithic contact, so it was classified as Paralithic Haplustoll.

Profile 2 (on the shoulder position) exhibits a very dark grayish brown A-horizon of 19 cm, with loamy texture and sub-angular block structure. Down in the profile, a transition AC-horizon of dark brown to brown color was identified. At 33 cm the C-horizon is dark yellow-brown. A mollic epipedon was recognized in this profile, but as it does not present a subsoil horizon it was classified as Entic Haplustoll.

Profile 3 (on the backslope position) has a very dark grayish brown topsoil of 22 cm, with a silty loam texture and sub-angular block structure (Fig. 2). Down in the profile, a silty loam, yellow-brown B-horizon of 26 cm with fine clay coatings and scarce clayskins was recognized. Finally, a C-horizon with free $CaCO_3$ disseminated in the mass was identified. This profile exhibits a mollic epipedon, but it does not present a subsoil horizon, hence it was classified as Udic Haplustoll. According to the *catena* position, this profile shows evidences of slight erosion by water.

Profile 4 (on the toeslope position) is the most developed soil of the *catena* and it is characterized by an upper very dark grayish brown A-horizon of 25 cm, with a silty loam texture and sub-angular block structure. These features, along with its organic matter content (>1%), and the base saturation > 50%, indicate that it is a mollic epipedon. Then, a Bt_1-horizon with abundant thick clay skins is found. At a depth of 56 cm a Bt_2-horizon is recognized, with scarce fine clay coatings and an irregular structure with strong to moderate prisms. The calculated clay ratio B/A (>1.2) indicates that this is an argillic horizon. At a depth of 86 cm, a BC-horizon with weak to massive blocks structure and few clay coatings is observed. This soil was classified as Udic Argiustoll.

The parent material of these soils is texturally classified as sandy loess for profiles 4 and 2, and as typical loess for profile 3, according to Pye (1995). On the other hand, as it was mentioned above, profile 1 exhibits a paralithic contact at 20 cm depth and it is develop over the Estancia Belgrano Formation.

The most noticeable pedogenetic processes in the profiles are decarbonatation-carbonatation, melanization, and argilluviation. Melanization was recognized in all profiles, whereas decarbonatation–carbonatation was identified through the presence of calcium carbonate in the C-horizons of profiles 3 and 2 (Table 1). Although carbonates in the studied soils have an aeolian origin (Dorronsoro and Aguilar, 1988), i.e., they are inherited from the parent material; their accumulation in the C-horizons is the result of contrasting climatic seasons, as occurs in the study area, that promote the dissolution-precipitation processes. Finally, the material removed from the upper horizons of profiles 3 and 4 is accumulated in the Bw- and Bt-horizons through the process of argilluviation. Clay coatings are clearly visible in the Bt-horizon and barely perceptible in the Bw-horizon.

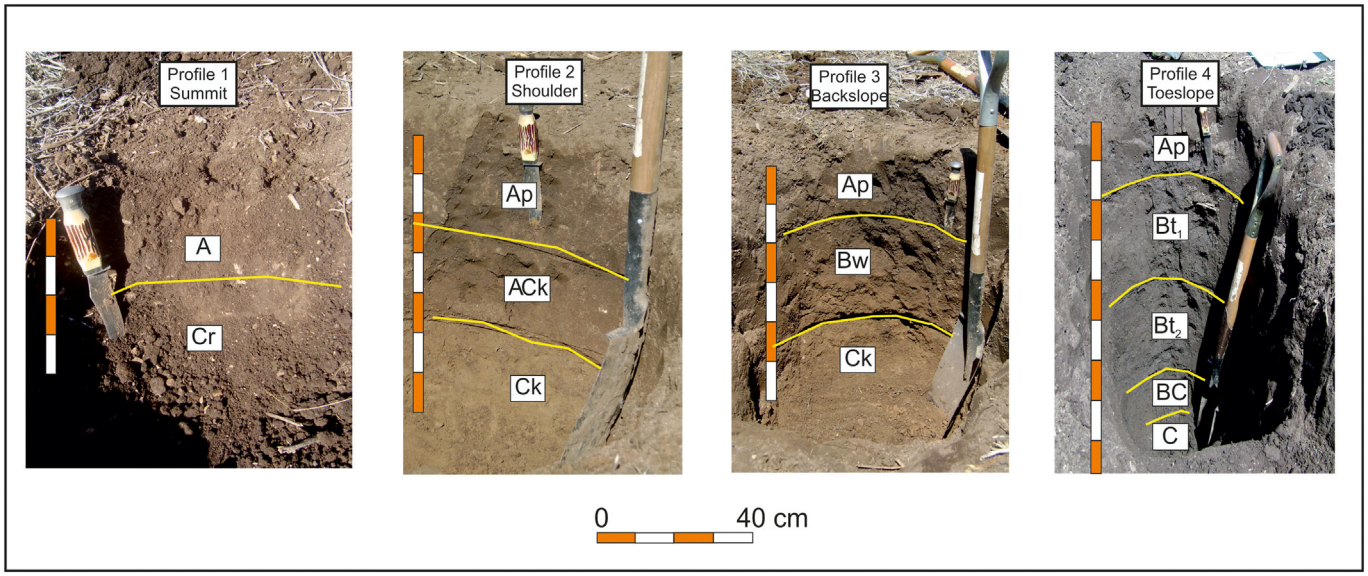

Fig. 2. Profile development and soil morphology of the studied *catena*.

Table 1
Soil properties and physico-chemical parameters for the studied *catena*.

Horizon	Depth	Color	Structure	Grain size							pH	EC	OC	$CaCO_3$	CE (cmol kg^{-1})				CEC	BS
	(cm)	(moist)		VCS	CS	MS	FS	VFS	Silt	Clay	(1:2.5)	($dS.m^{-1}$)	%	%	Ca^{+2}	Mg^{+2}	Na^{+}	K^{+}	(cmol kg^{-1})	(%)
Profile 1 (Summit): Paralithic Haplustoll, fine loam, thermic																				
A	0–20	10YR 3/1	Weak fine subangular blocky	12.1	11.3	6.8	4.9	3.8	35.9	24.5	8.3	0.24	2.8	1.6	n.d.	n.d.	0.3	1.3	25.4	100
Cr	>20	10YR 3/2																		
Profile 2 (Shoulder): Entic Haplustoll, fine loam, thermic																				
Ap	0–19	10YR 3/2	Moderate weak subangular blocky	2.5	5.8	5.7	6.1	7.0	50.1	23.0	7.0	0.16	1.6	_	13.3	0.9	0.3	1.3	17.00	92.5
ACk	19–33	10YR 4/3	Moderate medium subangular blocky	2.6	5.5	5.5	5.6	5.0	54.5	18.7	7.2	0.11	0.9	0.2	15.2	1.2	0.3	1.0	18.4	96.5
Ck	>33	7.5YR 5/4	massive	2.0	4.9	4.9	5.2	4.6	53.8	22.2	8.4	0.18	n.d.	8.1	n.d.	n.d.	0.2	0.8	19.00	100.0
Profile 3 (Backslope): Udic Haplustoll, fine loam, thermic																				
Ap	0–22	10YR 3/2	Moderate medium subangular blocky	3.0	6.2	5.4	5.3	5.6	52.1	22.4	6.9	0.08	1.2	_	11.9	1.2	0.3	1.3	15.9	92.6
Bw	22–48	10YR 3/4	Moderate medium subangular blocky	3.1	4.8	4.2	4.2	6.0	53.7	23.8	7.0	0.12	0.7	_	13.6	1.4	0.2	0.8	16.8	95.3
Ck	>48	7.5YR 5/4	Massive	2.6	4.2	3.4	3.5	5.9	57.0	23.4	8.5	0.16	n.d.	6.6	n.d.	n.d.	0.2	0.5	17.3	100.0
Profile 4 (Toeslope): Udic Argiustoll, fine loam, thermic																				
Ap	0–25	10YR 3/2	strong Medium subangular blocky	3.9	7.0	5.9	6.5	5.3	48.5	20.5	6.8	0.14	1.3	_	14.1	2.0	0.3	0.8	19.0	90.4
Bt_1	25–56	10YR 3/2	Strong medium irregular prismatic	7.3	8.1	8.0	7.5	4.2	35.0	29.5	7.0	0.06	0.6	_	16.9	1.5	0.5	1.2	20.6	97.6
Bt_2	56–86	10YR 4/2	Moderate medium irregular prismatic	9.8	9.1	9.8	8.5	3.8	32.6	24.4	7.0	0.06	n.d.	trace	14.0	2.0	0.2	0.9	17.9	95.7
BC	86–100	7.5YR 4/2	Weak very fine blocky to massive	9.8	9.2	7.9	5.4	3.1	36.1	25.2	7.2	0.05	n.d.	trace	15.0	2.8	0.3	0.6	18.9	98.7
C	>100	7.5YR 4/2	Massive	3.2	5.3	7.6	8.8	7.9	44.5	19.4	7.0	0.05	n.d.	_	14.2	2.9	0.3	0.5	19.0	94.0

VCS: very coarse sand; CS: coarse sand; MS: medium sand; FS: fine sand; VFS: very fine sand; EC: electrical conductivity; OC: organic carbon; CE: Cation exchange; CEC: Cation-exchange capacity; BS: base saturation; n.d.: not detected.

3.2. Soil geochemistry

The concentrations of major and trace elements, as well as of rare earth elements (REE), measured in the genetic horizons of the four analyzed profiles are shown in Tables 2 and 3 respectively. Several geochemical parameters are also included in the tables.

Geochemical datasets are multivariate (i.e., each sample has several major, trace and rare earth elements), thus the main difficulty in assessing multi-element data is multi-dimensional visualization. Several techniques can be employed, including the multi-element diagrams or spidergrams, which plot values for a range of elements in each sample, and involve normalizing the data to a reference (McQueen, 2009). The main advantage of these diagrams is the easy determination of element mobility to constrain weathering and pedogenic processes. As the provenance of clastic sediments is generally dominated by recycled upper crust materials, implying a mixture of the outcropping rocks on a large scale (e.g., Taylor and McLennan, 1985; McLennan, 1989), the chemical composition of sedimentary rocks is considered to reflect the approximate composition of the UCC. Therefore, in order to characterize the chemical composition of the different studied soils and their parent materials, the upper continental crust (UCC; McLennan, 2001) normalized diagrams or *spidergrams* of major and trace elements (Fig. 3) and rare earth elements (Fig. 4) were employed. Similar tools were used, for instance, by Caspari et al. (2006).

Fig. 3 shows the UCC-normalized extended patterns of major and trace elements for the bulk samples of profiles 2, 3 and 4, as well as the comparison of the C-horizons mean composition with loess from Argentina and other parts of the world. The UCC-normalized diagrams of the <62.5 μm size-fractions were not included in the figure as they exhibit similar patterns when compared to the bulk samples. The *X*-order of elements in the diagrams corresponds to the progressive enrichment of elements, from Ni to Cs, in the UCC with respect to the Earth's primitive mantle (Hofmann, 1988).

According to Figs. 3a, b and c, the analyzed soils show, in general, compositions similar to UCC, with the exception of some elements that exhibit increased or decreased concentrations when compared to the UCC. On the other hand, no major geochemical variations were recorded in the studied soil profiles, with the exception of profile 4 which shows slight differences. Major elements such as Al, Ti and Si, as well as, some trace elements such as Rb, Ba, Ta and Y show, in all profiles, similar concentrations than the UCC. Conversely, Ca, Na, K and Mg, which are mobile during chemical weathering, are slightly depleted. Ca, Na, and K reflect, in general, the weathering of feldspars, whereas the loss of Mg is likely associated with the alteration of clay minerals. Fe, V, Co, Cr, and Ni also exhibit depletions in all profiles compared to UCC (Fig. 3a, b and c), which can be associated with the alteration of pyroxenes and amphiboles. On the other hand, all profiles show an enrichment of As compared to UCC, an element that is abundant in the volcanic glass of the Pampean loess and groundwaters hosted in the aquifers (Nicolli et al., 2010). Thus, the enrichment of As in these soils is, undoubtedly, a feature inherited from the parent material. Cs is also enriched in the studied soils when compared to UCC (Fig. 3a, b and c), which reflects that this trace element is possible bound by micaceous minerals, such as illite (e.g., Hinton et al., 2006).

Although bulk samples of profiles 2 and 3 (on shoulder and backslope positions) have different genetic horizons, they do not display significant geochemical variations since their UCC-normalized patterns are very similar (Fig. 3a and b). On the contrary, profile 4 exhibits lower concentrations of U, Zr, Sr and Hf when compared to the other soils (Fig. 3c). The geochemical distribution of Sr is usually similar to

that of Ca (e.g., Middelburg et al., 1988), suggesting the alteration of plagioclase. On the other hand, depletions in Zr, Hf and U are likely associated with the sorting of accessory minerals resistant to weathering, such as zircon. Besides, profile 4 exhibits a larger geochemical variability along the different horizons compared to the other soils of the *catena* (Fig. 3c). Several textural variations were also recognized in this profile

Table 2
Major oxides and trace elements concentration, weathering indices and elemental ratios in the bulk samples and fine fractions for the studied soil profiles.

Geochemical parameter	Detection limit	Profile 1	Profile 2			Profile 3			Profile 4				
		Summit	Shoulder			Backslope			Toeslope				
		A	Ap	AC	Ck	Ap	Bw	Ck	Ap	Bt_1	Bt_2	BC	C
Bulk sample													
SiO_2	0.01	69.51	70.03	69.42	67.51	69.88	69.34	67.21	68.78	68.38	68.87	66.20	68.94
Al_2O_3	0.01	15.48	15.39	15.70	16.16	15.56	15.74	16.28	16.01	16.11	15.70	16.73	15.70
Fe_2O_3	0.04	4.60	4.68	4.57	5.01	4.66	4.79	5.32	5.42	5.29	4.90	6.00	4.85
MgO	0.01	1.38	1.33	1.40	1.77	1.30	1.36	1.72	1.69	1.77	1.79	2.20	1.78
CaO	0.01	2.97	2.46	2.67	3.25	2.43	2.57	3.23	2.04	2.52	2.89	2.83	2.91
Na_2O	0.01	2.61	2.76	2.88	2.66	2.77	2.80	2.63	2.14	2.25	2.43	2.23	2.41
K_2O	0.01	2.46	2.41	2.41	2.56	2.45	2.43	2.56	2.85	2.70	2.58	2.80	2.53
TiO_2	0.01	0.71	0.74	0.75	0.80	0.75	0.75	0.80	0.77	0.70	0.61	0.75	0.64
MnO	0.01	0.07	0.06	0.06	0.08	0.07	0.07	0.07	0.07	0.10	0.08	0.10	0.07
P_2O_5	0.01	0.21	0.13	0.14	0.20	0.13	0.14	0.17	0.21	0.19	0.14	0.16	0.15
Cs	0.1	5.5	5.7	5.6	6.2	5.8	5.8	7.8	8.8	7.3	6.8	8.1	6.5
Rb	0.1	88.4	93.4	91.2	92.7	94.3	91.2	99.1	120.7	108.5	102.1	115.8	100.3
U	0.1	2.2	2.7	2.5	2.4	2.6	2.6	2.1	2.2	2.5	1.9	2.4	1.8
Th	0.2	10.7	11.3	12.4	12.1	11.7	11.2	11.2	10.8	9.9	7.5	10.1	8.5
Ba	1	439	501	523	544	517	497	531	558	530	533	560	513
Ta	0.1	0.9	1.1	1.1	1.1	1.1	0.9	1.0	1.0	1.0	1.0	1.0	1.1
Zr	0.1	248.5	295.7	336.1	299.8	295.9	294.1	283.0	177.5	153.1	151.7	176.1	168.3
Hf	0.1	7.3	7.5	8.7	7.7	8.9	7.6	7.9	5.3	3.4	4.2	4.8	4.4
Sr	0.5	252.1	320.6	345.8	332.9	315.3	315.3	314.0	256.0	234.7	225.6	219.8	234.8
As	0.5	9.40	5.5	5.6	8.6	5.3	5.3	6.8	4.7	4.2	3.2	3.0	2.6
Zn	1	48.0	47.0	43.0	48.0	52.0	48.0	56.0	85.0	70.0	72.0	83.0	66.0
V	8	57.0	72.0	71.0	72.0	70.0	74.0	80.0	77.0	73.0	71.0	82.0	72.0
Co	0.2	7.90	8.9	8.2	9.6	9.0	8.5	10.2	9.8	11.5	10.3	13.1	10.4
Cr	2	28.79	32.7	27.4	34.0	27.4	38.5	50.1	33.4	33.0	33.0	39.0	27.3
Ni	0.1	11.0	10.6	10.3	11.7	8.6	13.4	15.1	12.0	14.3	14.0	15.8	12.9
Y	0.1	24.0	25.8	27.5	27.1	27.1	28.5	26.2	25.5	23.7	22.6	26.5	22.0
CIA		56.06	57.28	56.57	55.51	57.55	57.25	56.04	61.28	59.41	56.91	58.95	57.04
ICV		1.28	1.24	1.26	1.35	1.22	1.24	1.34	1.20	1.25	1.31	1.33	1.31
Ba/Sr		1.74	1.56	1.51	1.63	1.64	1.58	1.69	2.18	2.26	2.36	2.55	2.18
Rb/Sr		0.35	0.29	0.26	0.28	0.30	0.29	0.32	0.47	0.46	0.45	0.53	0.43
Fine fraction (<62.5 mm)													
SiO_2	0.01	69.02	69.39	68.74	66.95	67.64	68.61	66.55	64.31	67.58	63.92	63.78	65.06
Al_2O_3	0.01	15.18	15.29	15.72	16.39	16.50	16.11	16.50	18.29	15.86	16.93	16.96	16.64
Fe_2O_3	0.04	4.99	5.16	4.92	5.43	5.72	5.07	5.63	7.68	6.16	7.90	7.97	7.30
MgO	0.01	1.40	1.43	1.49	1.87	1.65	1.42	1.81	2.32	1.98	2.86	2.90	2.53
CaO	0.01	2.94	2.39	2.62	2.92	2.16	2.43	3.27	1.56	2.20	2.19	2.24	2.20
Na_2O	0.01	2.78	2.78	2.92	2.68	2.47	2.78	2.56	1.35	2.12	1.72	1.64	1.87
K_2O	0.01	2.50	2.47	2.49	2.58	2.72	2.50	2.54	3.22	2.83	3.08	3.13	3.06
TiO_2	0.01	0.93	0.90	0.88	0.88	0.92	0.88	0.87	0.87	0.92	1.07	1.06	1.02
MnO	0.01	0.07	0.07	0.07	0.08	0.09	0.07	0.07	0.11	0.11	0.12	0.12	0.11
P_2O_5	0.01	0.20	0.13	0.14	0.22	0.14	0.13	0.18	0.30	0.23	0.20	0.20	0.21
Cs	0.1	6.0	6.8	6.9	6.6	7.8	6.5	7.2	12.1	9.1	10.7	10.8	10.7
Rb	0.1	90.1	98.9	93.0	94.9	110.6	97.9	102.8	142.4	118.4	148.7	142.6	138.7
U	0.1	3.1	2.5	2.5	2.6	2.6	2.5	2.4	2.6	2.9	2.9	2.9	2.6
Th	0.2	12.4	12.4	12.1	12.9	12.9	12.3	13.1	15.3	12.9	14.7	15.3	15.1
Ba	1	498	547	534	532	517	534	542	479	530	575	548	555
Ta	0.1	1.2	1.4	1.0	1.2	1.1	1.3	1.1	1.2	1.2	1.4	1.3	1.4
Zr	0.1	418.5	381.8	394.6	350.8	298.6	347.6	327.2	165.3	257.8	217.6	224.0	293.0
Hf	0.1	9.8	9.5	10.0	9.3	8.3	9.1	9.9	4.1	6.5	6.6	5.7	7.8
Sr	0.5	307.6	341.4	361.6	338.1	295.3	345.4	330.2	186.3	258.0	208.7	199.5	221.8
As	0.5	8.2	7.1	7.2	9.1	7.6	7.2	6.4	7.4	5.0	4.1	3.9	4.6
Zn	1	43.0	51.0	43.0	47.0	56.0	50.0	54.0	127.0	81.0	108.0	101.0	86.0
V	8	81.0	76.0	76.0	83.0	74.0	79.0	84.0	81.0	81.0	100.0	102.0	94.0
Co	0.2	8.6	9.5	9.4	10.8	10.5	9.2	11.3	13.8	11.9	17.2	16.7	15.1
Cr	2	39.7	43.6	38.3	45.9	27.8	38.9	33.3	34.1	39.0	50.9	56.7	44.4
Ni	0.1	10.0	10.7	11.9	13.0	12.7	14.4	14.0	18.9	16.1	22.8	25.3	19.2
Y	0.1	30.1	28.5	28.0	28.1	28.3	27.2	30.8	30.3	30.1	32.0	32.7	30.8
CIA		55.0	57.2	56.5	56.3	60.5	58.2	56.5	68.8	60.5	63.0	63.0	62.1
ICV		1.36	1.29	1.30	1.34	1.21	1.23	1.35	1.13	1.31	1.42	1.42	1.38
Ba/Sr		1.62	1.60	1.48	1.57	1.75	1.55	1.64	2.57	2.05	2.76	2.75	2.50
Rb/Sr		0.29	0.29	0.26	0.28	0.37	0.28	0.31	0.76	0.46	0.71	0.71	0.63

Major oxides concentrations are in % and recalculated to 100% free of volatile.
Trace elements concentrations are in ppm.
CIA: Chemical Index of Alteration, ICV: Index of Compositional variability.

(Table 1) as it exhibits a higher percentage of the sand fraction. This fact, along with the geochemical differences mentioned above, could indicate another source of material for this profile in addition to loess, i.e., alluvial material from the crystalline basement and from the Estancia Belgrano Formation.

Although some geochemical features of the analyzed soils can be attributed to chemical alteration (e.g., depletion in soluble elements compared to UCC), it can be to assumed that they are mainly inherited. In order to compare the parent material (i.e., C-horizons mean composition) with other loess from Argentina, the UCC-normalized extended diagram of Fig. 3d is presented. Data of loess from other regions of the world are also included for comparison. It can be seen in Fig. 3d that the mean composition of C-horizons displays roughly a similar pattern compared to other loess from Argentina (i.e., Pampean, Buenos Aires and Ancasti range loess). In general, some trace elements such as Cs, Th, Ta, Zr, As and Y are enriched with respect to the UCC, indicating the concentration of illite (Cs), heavy minerals like rutile and zircon (Th, Ta and Zr), volcanic glass (As) and Mn-oxides (Y). Conversely, the depletions in K, Sr, Na and Ca are likely associated with the chemical alteration of feldspars, whereas the weathering of amphiboles is evidenced by depletions in Rb, V, Co, Cr and Ni. Besides, the C-horizons of the studied soils and loess from Argentina are depleted in Mg and U, suggesting the alteration of micas and apatite respectively, since they are elements commonly hosted in these primary minerals (e.g., Scott, 2009), which are present in the loessic sediments.

The REE concentration in soils is mainly controlled by the mineralogical composition of the parent material. REE are especially adequate as tracers since they are evenly distributed in minerals, they mainly come from the parent materials with restricted anthropogenic sources, and they evolve as a group, although processes induce internal fractionations and/or anomalies (Laveuf and Cornu, 2009). On the other hand, human activities, such as P-fertilization, can be responsible for minor REE inputs into soils (Aubert et al., 2002). Several examples of the use of REE as indicators of pedogenic processes are those of Caspari et al. (2006), Laveuf and Cornu (2009, and references therein), Marques et al. (2012), among others. Hu et al. (2006) distinguished two major

Table 3
Rare earth elements (REE) concentration and related parameters in the studied soil profiles.

Geochemical parameters	Detection limit	Bulk sample											
		Profile 1	Profile 2			Profile 3			Profile 4				
		Summit	Shoulder			Backslope			Toeslope				
		A	Ap	AC	Ck	Ap	Bw	Ck	Ap	Bt_1	Bt_2	BC	C
La	0.10	29.7	31.8	32.3	32.2	32.0	30.5	33.3	32.4	31.1	30.6	40.1	30.4
Ce	0.10	59.8	65.6	64.6	66.7	64.9	61.4	66.5	67.3	62.1	59.8	76.8	58.9
Pr	0.02	7.15	7.46	7.76	7.86	7.81	7.39	7.93	7.83	7.50	7.13	8.95	7.16
Nd	0.30	27.1	30.9	32.8	30.2	31.7	30.5	29.2	30.1	30.2	28.8	35.5	27.6
Sm	0.05	5.14	5.75	5.79	6.11	5.88	5.78	6.17	6.04	5.68	5.32	6.38	5.48
Eu	0.02	1.07	1.10	1.19	1.25	1.20	1.21	1.19	1.23	1.19	1.12	1.36	1.17
Gd	0.05	4.41	4.98	5.26	5.31	5.10	5.15	5.10	5.28	5.19	4.72	5.63	4.85
Tb	0.01	0.74	0.77	0.83	0.84	0.81	0.82	0.81	0.84	0.77	0.74	0.90	0.75
Dy	0.05	4.51	4.76	5.51	4.73	5.40	5.07	4.48	4.72	4.23	4.29	4.97	3.86
Ho	0.02	0.88	0.90	0.97	0.96	1.08	1.01	0.95	0.94	0.98	0.83	0.98	0.79
Er	0.03	2.51	2.66	3.32	2.83	2.93	2.89	2.91	2.84	2.56	2.42	2.78	2.29
Tm	0.01	0.39	0.39	0.48	0.43	0.45	0.50	0.40	0.38	0.35	0.35	0.40	0.35
Yb	0.05	2.22	2.73	2.88	2.76	2.93	3.32	2.83	2.63	2.13	2.05	2.60	2.27
Lu	0.01	0.39	0.42	0.48	0.45	0.45	0.48	0.47	0.46	0.39	0.33	0.40	0.33
ΣREE		146.0	160.2	164.2	162.6	162.6	156.0	162.2	163.0	154.4	148.5	187.8	146.2
ΣLREE		123.8	135.8	137.5	137.0	136.4	129.8	136.9	137.6	130.9	126.3	161.4	124.1
ΣMREE		15.9	17.4	18.6	18.2	18.4	18.0	17.8	18.1	17.1	16.2	19.2	16.1
ΣHREE		6.39	7.1	8.13	7.43	7.84	8.2	7.56	7.25	6.41	5.98	7.16	6.03
La_N/Yb_N		0.98	0.85	0.82	0.86	0.80	0.67	0.86	0.90	1.07	1.09	1.13	0.98
Eu_N/Eu_N^*		1.06	0.97	1.01	1.03	1.03	1.04	1.00	1.02	1.03	1.05	1.07	1.07
Ce_N/Ce_N^*		0.93	0.93	0.89	0.95	0.91	0.90	0.93	0.95	0.90	0.89	0.89	0.89
Fine fraction (<62.5 mm)													
La	0.10	34.1	33.0	32.9	34	34.5	31.5	35.0	41.8	38.4	51.4	51.5	47.3
Ce	0.10	72.7	66.0	64.3	71.2	69.6	67.8	71.1	84.9	73.6	96.4	100.5	92.3
Pr	0.02	8.06	7.71	7.97	8.27	8.26	7.9	8.37	9.96	8.87	11.59	11.54	10.78
Nd	0.30	34.7	31.9	32.8	33.5	32.4	30.7	32.5	41.4	35.9	45.7	44.6	42.9
Sm	0.05	6.23	5.89	5.67	6.08	6.02	5.86	6.43	7.63	6.52	7.91	7.94	7.49
Eu	0.02	1.22	1.12	1.28	1.22	1.19	1.23	1.22	1.45	1.34	1.48	1.54	1.47
Gd	0.05	5.49	5.45	4.96	5.69	5.42	4.99	5.49	6.41	5.68	6.82	6.88	6.74
Tb	0.01	0.88	0.84	0.83	0.88	0.87	0.82	0.86	1.02	0.90	1.05	1.08	1.00
Dy	0.05	5.2	5.34	5.13	4.88	4.93	4.47	4.94	5.84	5.30	5.61	6.00	5.52
Ho	0.02	1.13	1.11	0.98	1.00	0.94	0.96	0.96	1.09	0.98	1.17	1.12	1.09
Er	0.03	3.13	3.15	2.87	3.32	3.23	3.01	3.42	3.31	3.10	3.60	3.39	3.23
Tm	0.01	0.48	0.45	0.45	0.42	0.46	0.46	0.48	0.46	0.49	0.45	0.48	0.47
Yb	0.05	3.5	3.22	3.14	3.18	3.14	3.38	3.33	3.04	2.82	3.10	2.93	3.11
Lu	0.01	0.47	0.52	0.51	0.5	0.48	0.49	0.47	0.46	0.46	0.50	0.51	0.48
ΣREE		177.3	165.7	163.8	174.1	171.4	163.6	174.6	208.8	184.4	236.8	240.0	223.9
ΣLREE		149.6	138.6	138.0	147.0	144.8	137.9	147.0	178.1	156.8	205.1	208.1	193.3
ΣMREE		19.0	18.6	17.9	18.8	18.4	17.4	18.9	22.4	19.7	22.9	23.4	22.2
ΣHREE		8.71	8.45	7.95	8.42	8.25	8.3	8.66	8.36	7.85	8.82	8.43	8.38
La_N/Yb_N		0.71	0.75	0.77	0.78	0.81	0.68	0.77	1.01	1.00	1.22	1.29	1.12
Eu_N/Eu_N^*		0.98	0.93	1.13	0.97	0.98	1.07	0.96	0.97	1.03	0.95	0.98	0.97
Ce_N/Ce_N^*		0.94	0.90	0.87	0.94	0.92	0.97	0.93	0.91	0.88	0.87	0.91	0.90

$Eu_N/Eu_N^* = Eu/(Sm * Gd)^{0.5}$ (McLennan, 1989).
$Ce_N/Ce_N^* = Ce/(1/3Nd + 2/3La)$ (Elderfield et al., 1990).
N denotes normalization to Upper Continental Crust (McLennan, 2001).

types of parent materials based on their REE content: a) acid or basic igneous rocks, sandstones and shales; and b) loess and calcareous rocks. These authors stated that loess and calcareous rocks have a ΣREE that ranges from 137 to 174 ppm. The analyzed soils exhibit REE contents within this range, between ~146 and ~188 ppm (Table 3).

Fig. 4 shows the UCC-normalized REE *spidergrams* for the analyzed soil profiles. In this case, the diagrams for the bulk samples and the <62.5 μm size-fractions were included in the figure. According to Fig. 4 the bulk samples and the <62.5 μm size-fractions are generally enriched in REE compared to the UCC. Profiles 2 and 3 exhibit similar

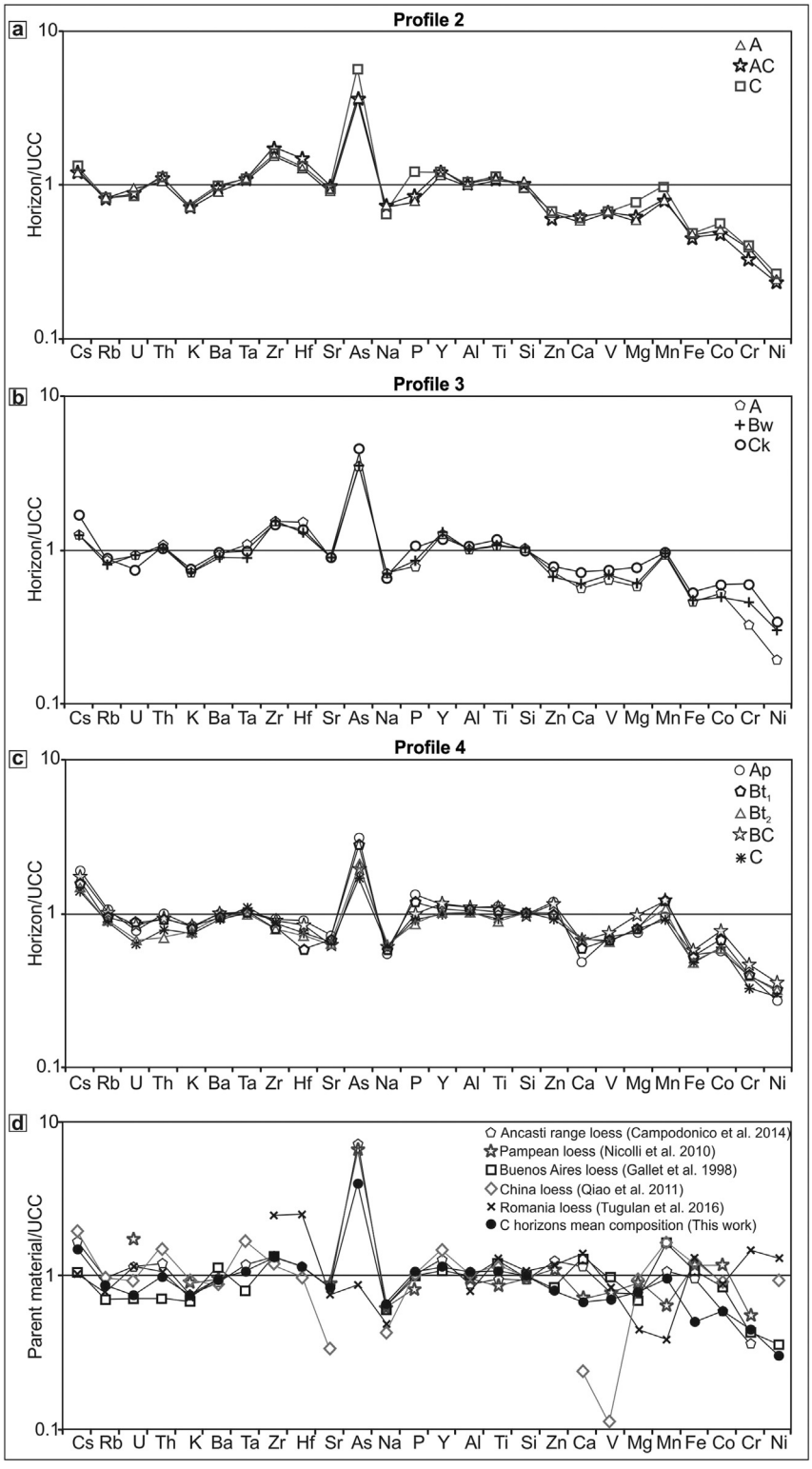

Fig. 3. a) UCC-normalized extended diagram of the bulk samples of profile 2 (located on shoulder position), b) Idem for profile 3 (on the backslope position), c) Idem for profile 4 (on the toeslope positions), d) UCC-normalized extended diagram for C-horizons mean composition of the studied soils. Loess composition of Argentina and other regions of the world are included for comparison. Elements are ranked on the X-axis according to their progressive enrichment in the upper continental crust (UCC, McLennan, 2001) with respect to the Earth's primitive mantle (Hofmann, 1988).

REE-patterns with enrichments in heavy rare earth elements (HREE; from Dy to Lu), which are also evidenced by La_N/Yb_N ratios (where N denotes normalization to UCC) ranging from 0.67 to 0.86 (Table 3). These profiles also show a middle rare earth elements (MREE; from Nd to Tb) enrichment (Fig. 4a, b, d and e). The high HREE content is probably associated with the presence of heavy minerals, such as zircon, which are rather stable during weathering, whereas the MREEs enrichment is likely caused by the occurrence of phosphate minerals (e.g., Hannigan and Sholkovitz, 2001) or Fe-Mn oxyhydroxides (e.g., Johanesson and Zhou, 1999) in the analyzed soils. Furthermore, the presence of organic matter complexes with HREEs and MREEs could be responsible for the observed enrichments (e.g., Aubert et al., 2001).

Fig. 4c and f show that profile 4 exhibits different REEs UCC-normalized patterns in comparison with profiles 2 and 3. Besides, some differences can be found between the bulk samples and the <62.5 μm size-fractions of the genetic horizons of this profile. Bulk samples of profile 4 show a MREE enrichment compared to UCC, with a pronounced convexity in the MREEs (Fig. 4c), whereas the <62.5 μm size-fractions of this profile exhibit an enrichment not only in MREEs (Fig. 4d) but also in LREEs (LREE; La to Nd) as it is evidenced by La_N/Yb_N ratios ranging between 1.00 and 1.29 (Table 3). Light REEs adsorb preferentially on Mn-oxides and phosphates (e.g., Laveuf and Cornu, 2009 and references therein). This variability does not appear to be a consequence of weathering or pedogenic processes. For instance, argilluviation usually produces a MREE transference along a soil profile (Laveuf and Cornu, 2009), but in this case there is not a surface horizon depleted in MREEs and a subsurface one enriched in MREEs. Therefore, the REE composition of the studied soils is likely (as in the case of trace elements) inherited from the parent material. In the case of profile 4, the REE content also indicates a local source of material in addition to the loess.

Fig. 5 shows the HREE and LREE fractionation through the UCC-normalized La_N/Yb_N ratio for profiles 2, 3 and 4. REE fractionation is thought to be mainly controlled by the relative abundances of primary and secondary minerals (Nesbitt, 1979). It can be seen, in general, a progressive decrease in HREEs from profile 2 (on shoulder position) to profile 4 (on toeslope position). To explain the statistical relationship of the REE fractionation in the bulk samples and in the <62.5 μm size-fraction a regression model without intercept was used; the obtained regression lines are included in Fig. 5. The GAMLSS models revealed that the interaction between La_N and the two groups (i.e, bulk samples and fine fractions) was significant ($p < 0.001$), as well as, the main group effect ($p < 0.05$) and La_N ($p < 0.001$). For the bulk samples the adjusted

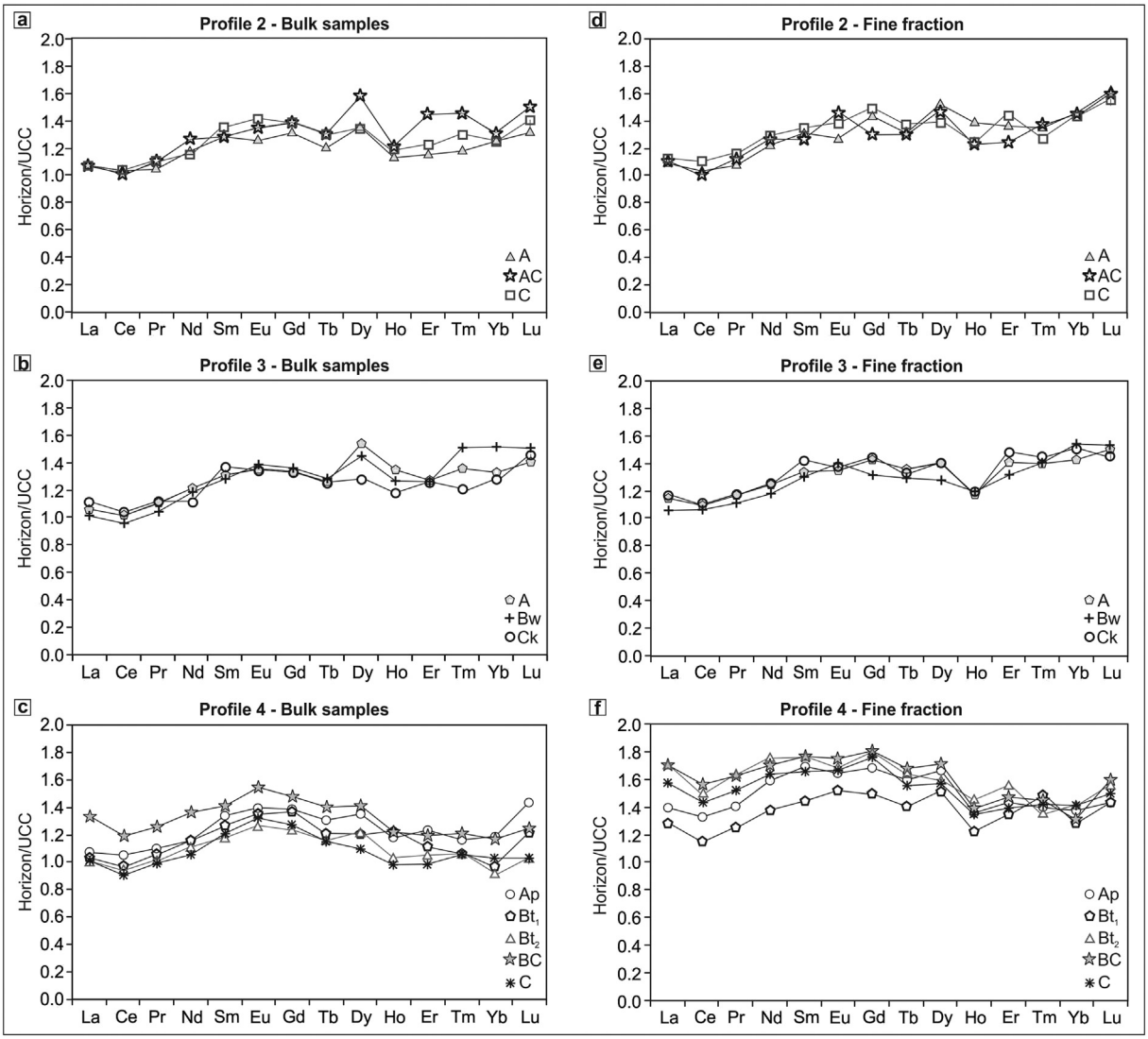

Fig. 4. a), b) and c) UCC-normalized REE spidergrams of the bulk samples of profiles 2, 3 and 4 located on shoulder, backslope and toeslope positions respectively. d), e) and f) Idem for the <62.5 μm size-fractions. The Y-axis has an arithmetic scale in order to easily identify the differences between the patterns. Upper continental crust (UCC) composition from McLennan (2001).

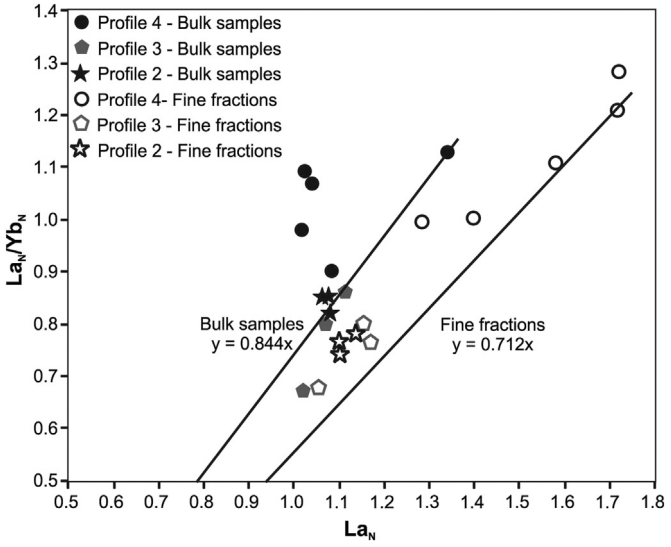

Fig. 5. La_N/Yb_N vs. La_N diagram showing the high rare earth elements (HREE) and light rare earth elements (LREE) fractionation for the bulk and <62.5 μm size-fraction samples of profiles 2, 3 and 4 located on shoulder, backslope and toeslope positions respectively. N denotes upper continental crust (UCC) normalization; UCC composition from McLennan (2001).

model is $Yb_N = e^{(0.6721-0.3885La_N)}$, so that, for instance, for a median La_N value of 1.1, the expected Yb_N is 1.277. On the other hand, for the fine fractions the adjusted model is $Yb_N = e^{(0.4805-0.0981La_N)}$, indicating in this case, for a median La_N value of 1.1 an expected Yb_N value of 1.451. These results indicate that the fine fraction (<62.5 μm) would be controlling the REEs fractionation in the analyzed soils.

The bulk and the <62.5 μm size-fraction samples collected at the different profiles all exhibit slightly negative Ce anomalies ($Ce_N/Ce_N^* = 0.87–0.97$; Table 3). Thus, no redox-controlled processes leading to CeO_2 precipitation seem to have occurred at the studied site. Furthermore, no significant Eu anomalies were identified in the analyzed samples ($Eu_N/Eu_N^* = 0.93–1.13$; Table 3).

The major, trace and REE composition of profiles 2, 3 and 4 were also normalized against the parent material (C-horizons) of their respective profiles (Fig. 6) with the aim of analyzing the mobility of elements through each profile, and to detect differences along the *catena*. The bulk samples of profiles 2 and 3 exhibit depletions in some soluble elements (Mg, Ca and P), which imply that these soils are poorly developed and barely affected by pedogenic processes (Fig. 6a and b). These soils are also slightly depleted in volcanic glass (As) and amphiboles (Co, Cr and Ni) when compared to C-horizon. Further, slightly enrichments in HREE are observed in the surface and subsurface horizons of both profiles (Fig. 6d and e), which is likely associated with the presence of heavy minerals, such as zircon.

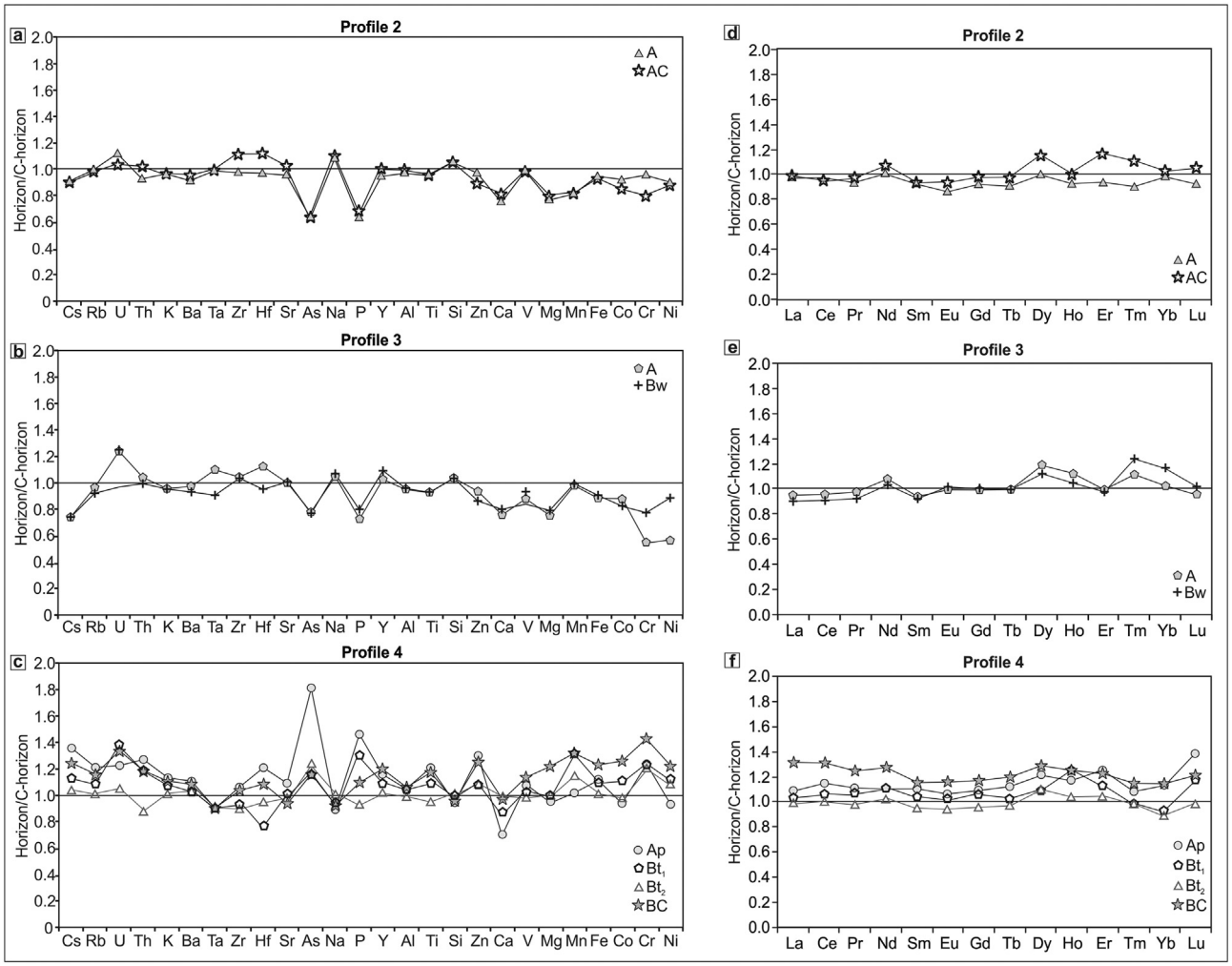

Fig. 6. a), b) and c) Multielemental C-horizon-normalized diagrams of the bulk samples of profiles 2, 3 and 4 located on shoulder, backslope and toeslope positions respectively. Elements are ranked on the X-axis according to their progressive enrichment in the upper continental crust (UCC, McLennan, 2001) with respect to the Earth's primitive mantle (Hofmann, 1988). d), e) and f) C-horizon-normalized REE diagrams of the bulk samples of the same profiles. The Y-axis has an arithmetic scale in order to easily identify the differences between the patterns.

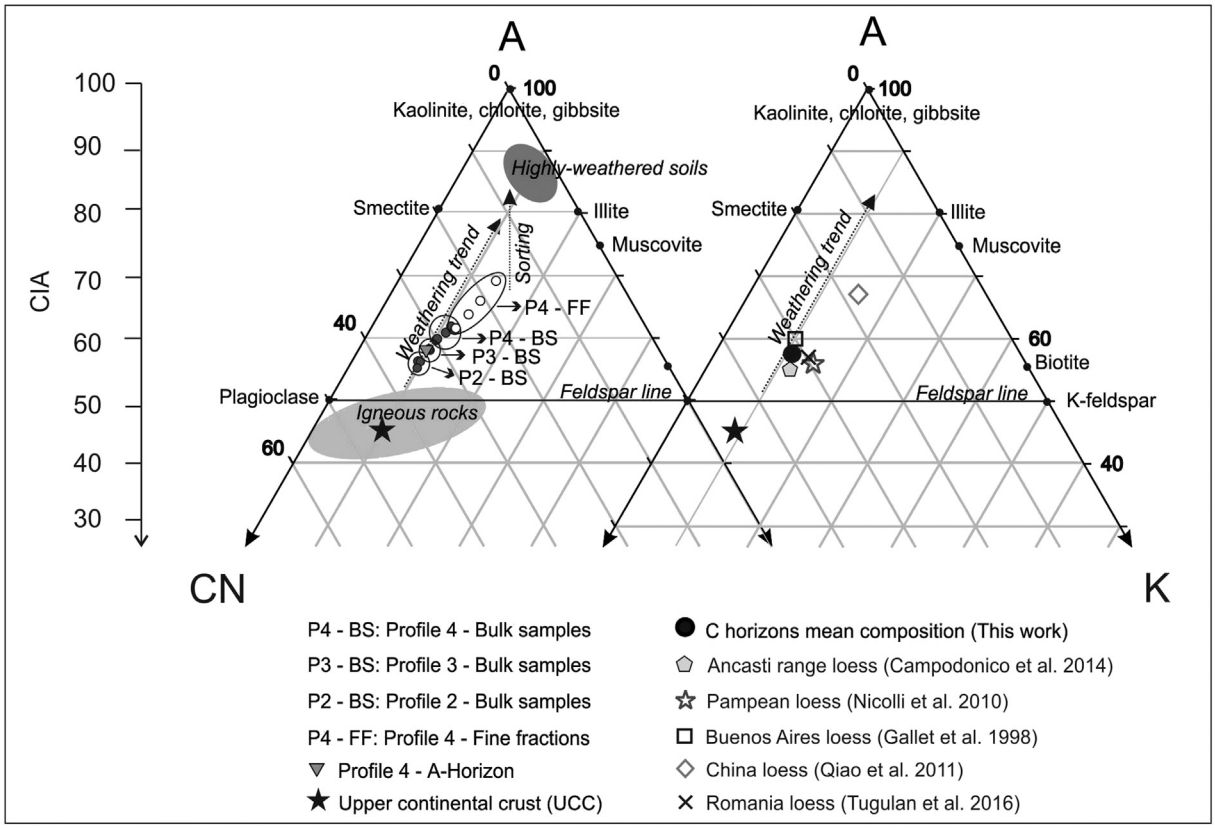

Fig. 7. A-CN-K ternary diagrams for the studied soil profiles (diagram on the left) and the parent material, as well as loess from Argentina and other regions of the world (diagram on the right). The supplementary vertical axis of CIA, the upper continental crust (UCC) composition, and the theoretical weathering and sorting trends are also included. The fields of igneous rocks and highly weathered soils (from Caspari et al., 2006) are plotted for comparison. The UCC composition is from McLennan (2001).

On the contrary, the solum of profile 4 displays greater compositional changes compared to the C-horizon. In general, profile 4 is enriched in major and trace elements when compared to the parent material (Fig. 6c). Cs, U, Th, As, P, Mn, Fe, Co, Cr and Ni display the greater enrichments. REEs are also mobilized and fractionated as surface and subsurface horizons of profile 4 are enriched in REE when compared to the parent material (Fig. 6f). This variability indicates a larger intensity of the pedogenic processes in this soil, which can be associated with its landscape position, and the presence of a local source (i.e. alluvial material), the latter also evidenced in the grain-size of this profile (Table 1).

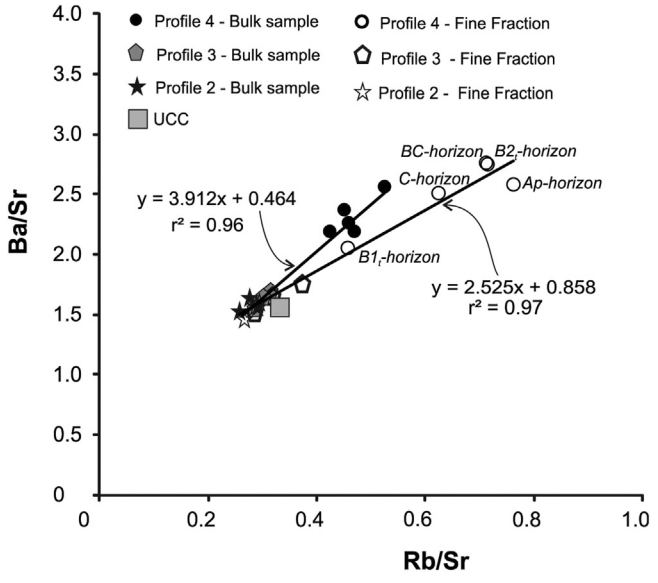

Fig. 8. Ba/Sr vs. Rb/Sr plot for profiles 2, 3 and 4 located on shoulder, backslope and toeslope positions respectively. The regression lines of these elemental ratios for the bulk and <62.5 μm size-fraction samples are also included. The horizons of profile 4 are indicated. Upper continental crust (UCC) composition from McLennan (2001).

3.3. Weathering imprint

During the early stages of pedogenesis, the chemical composition of soils is mainly controlled by the chemical composition of parental material, whereas the composition of mature soils reflects the effects of weathering. The divergence between the parent material and the resulting soils can be evident through a redistribution of elements between the different horizons of the profile, as well as through significant chemical variations between soils located in different landscape positions (e.g. Jenkins and Jones, 1980).

Several approaches may be conducted to establish the intensity of weathering processes. Among them, the geochemical proxies of mineral alteration, that is to say, weathering indices and elemental ratios, which have been widely used in the literature (e.g. Depetris et al., 2014 and references therein). In general, these indices compare the concentration of an immobile element with several mobile components. The most common index used to quantify the degree of weathering is the Chemical Index of Alteration (CIA, Nesbitt and Young, 1982). CIA is calculated in molar proportions as follows: $CIA = 100\ [Al_2O_3/(Al_2O_3 + CaO^* + Na_2O + K_2O)]$, where CaO^* represents the Ca in the silicate fraction only, adjusted for some other Ca-bearing minerals such as apatite and carbonates. The CIA quantitatively represents the degree to which the primary feldspars have been transformed into secondary clay minerals. The UCC has a mean CIA of 47, whereas highly weathered materials have values of >80, and clay minerals have CIAs close to 100. The CIA values for the studied soils are shown in Table 2. Because carbonates were previously eliminated in the soil samples, we only applied here the

Table 4
The Spearman's rank coefficients of selected major and trace elements for the bulk samples. The ΣREE is also included. Numbers in bold indicate a statistically significant correlation.

	Al	As	Ba	Ca	Cs	Fe	Hf	K	Mg	Mn	Na	Nb	Ni	Rb	Σ REE	Si	Sr	Th	Ti	U	V	Y	Zn	Zr
Al	1																							
As	−0.19	1																						
Ba	**0.7*****	−0.3	1																					
Ca	0.29	0.33	0.05	1																				
Cs	**0.74****	−0.56	**0.8****	−0.07	1																			
Fe	**0.82****	−0.42	**0.79****	0.06	**0.95***	1																		
Hf	−0.13	**0.67*****	−0.2	0.01	−0.45	−0.45	1																	
K	**0.64*****	−0.45	**0.76****	0.03	**0.9***	**0.9***	**−0.61*****	1																
Mg	**0.61*****	−0.52	**0.66*****	0.5	**0.62*****	**0.65*****	**−0.62*****	**0.68*****	1															
Mn	**0.73****	−0.44	**0.76****	0.1	**0.78****	**0.82****	−0.49	**0.85***	**0.7*****	1														
Na	−0.41	0.56	−0.54	0.02	**−0.76****	**−0.75****	**0.78****	**−0.9***	**−0.64*****	**−0.62*****	1													
Nb	0.45	0.22	0.35	−0.31	0.26	0.23	0.53	0.05	−0.24	0.03	0.14	1												
Ni	**0.73****	−0.46	0.46	0.29	**0.74****	**0.79****	−0.57	**0.69*****	**0.71*****	**0.75****	**−0.59*****	−0.02	1											
Rb	0.47	**−0.75****	**0.71****	−0.31	**0.91***	**0.81****	−0.59	**0.84***	0.57	**0.67*****	**−0.82****	0.08	0.57	1										
Σ REE	0.41	0.01	0.6	−0.31	0.29	0.27	0.46	0.1	−0.01	0.18	0.08	**0.8****	−0.08	0.24	1									
Si	**−0.94***	0.24	**−0.79****	−0.41	**−0.81****	**−0.88***	0.31	**−0.78****	**−0.78****	**−0.83***	0.57	−0.24	**−0.81****	−0.57	−0.27	1								
Sr	−0.25	**0.68*****	−0.29	−0.07	−0.57	−0.53	**0.82****	**−0.72****	**−0.64*****	**−0.61*****	**0.81***	0.4	**−0.7*****	**−0.66*****	0.31	0.44	1							
Th	−0.1	**0.69*****	−0.11	−0.1	−0.46	−0.41	0.9	**−0.6*****	**−0.6*****	−0.46	**0.75****	0.56	**−0.64*****	−0.57	0.55	0.3	**0.94***	1						
Ti	0.58	0.46	0.36	0.1	0.26	0.36	**0.59*****	0.09	−0.13	0.13	0.17	**0.81****	0.08	−0.08	**0.63*****	−0.41	0.47	**0.61*****	1					
U	−0.25	0.24	−0.31	−0.57	−0.43	−0.36	0.42	−0.52	**−0.68*****	−0.27	0.57	0.26	−0.43	−0.34	0.34	0.46	0.53	**0.6*****	0.15	1				
V	**0.81****	−0.32	0.53	−0.06	**0.77****	**0.83***	−0.21	0.55	0.37	0.53	−0.43	0.51	**0.74****	0.56	0.39	**−0.72****	−0.26	−0.16	0.55	−0.07	1			
Y	0.16	0.44	−0.02	−0.11	−0.29	−0.22	**0.79****	−0.46	−0.43	−0.14	**0.69*****	**0.66*****	−0.28	−0.47	**0.63*****	0.08	**0.68*****	**0.81****	**0.68*****	**0.63*****	0.11	1		
Zn	0.48	**−0.7****	**0.65*****	−0.15	**0.89***	**0.8****	**−0.64*****	**0.92***	**0.61*****	**0.75****	**−0.88***	−0.01	**0.65*****	**0.91***	0.06	**−0.61*****	**−0.81****	**−0.72****	−0.09	−0.53	0.49	−0.51	1	
Zr	−0.17	**0.7****	−0.22	−0.02	−0.57	−0.51	**0.92***	**−0.69*****	**−0.62*****	−0.55	**0.8****	0.47	**−0.69*****	**−0.67*****	0.47	0.38	**0.94***	**0.98***	0.55	**0.58*****	−0.24	**0.81****	**−0.79****	1

* $p < 0.001$.
** $p < 0.01$.
*** $p < 0.05$.

correction for apatite, using the concentrations of P_2O_5 as it was proposed by McLennan (1993). CIAs for the bulk samples range between ~56 and ~61, denoting incipient weathering. Although minimal differences of CIA values are registered along the *catena*, it is possible to note that profile 4 (on the toeslope position) shows the highest values (Table 2). This is consistent with its position in landscape, where a higher infiltration is possible so the soil retains a larger amount of water after rainfall, thus allowing the development of horizons (e.g., Porta-Casanellas et al., 2003). Also, along this profile is possible to distinguish variations in CIA values, whereas in the other soils almost no differences between the CIAs of A-horizons and those of the parent material can be recognized. As expected, the fine fractions have larger CIAs than the bulk samples, as a consequence of a minor grain size and a higher proportion of clay minerals. Again, profile 4 shows the highest values, with a CIA value of ~70 for the <62.5 μm size-fraction of A-horizon. It is also noticeable in this profile that CIA values do not decrease progressively in the soil profile as it would be expected, which could indicates water remobilization (by resuspension and redeposition) after the primary wind deposition of parent material (Argüello et al., 2012).

Another index frequently used to assess chemical alteration is the Index of Compositional Variability (ICV) proposed by Cox et al. (1995). ICV considers the abundance of alumina relative to other major oxides as follows: $ICV = (Fe_2O_3 + K_2O + Na_2O + CaO + MgO + MnO + TiO_2)/-Al_2O_3$. From the definition, it is clear that clay minerals have lower ICVs compared to non-clay silicates. In general, ICVs higher than 1.2 are typical of compositionally immature sediments, whereas mature sediments show ICVs < 1 (Cox et al., 1995). In the studied soils ICVs of bulk samples (Table 2) indicate a low chemical alteration, with a slightly increase in the values of the subsurface horizons (mean ICV for B-horizons: 1.28) compared to the surficial ones (mean ICV for A-horizons: 1.23). Mean ICV for parent materials (i.e., C-horizons) is 1.33. As in the case of the CIA, in the fine fraction the ICV values reflect the higher contents of clay minerals. Thus, the chemical indices used here suggest that the analyzed soils have been affected by a weak degree of weathering.

Ternary A-CN-K plot (Nesbitt and Young, 1989; Nesbitt et al., 1996) is another tool extensively used in the literature to evaluate the extent of chemical weathering. In this diagram, the theoretical composition of plagioclase (Pl) and K-feldspar (Kfs) plot at 50% of the Al_2O_3 apex, defining the "feldspar line", which represents the initial path to weathering. On the other hand, the theoretical composition of most clay minerals, which represent highly weathered materials, plot at the Al_2O_3 apex (Nesbitt et al., 1996). The vertical line on the left of the graph represents CIA values. Fig. 7 shows the ternary plots (A-CN-K) for the studied soils and loess from Argentina and other regions of the world. The fields of igneous rocks and highly weathered soils (Caspari et al., 2006) are also plotted for comparison. An increasing weathering trend can be distinguished from the shoulder position (profile 2) to the toeslope position (profile 4), and, as it was pointed out above, the most developed soil (i.e., profile 4) evidences the highest degree of chemical alteration (Fig. 7). The fine fractions (<62.5 μm) of profile 4 plot towards more weathered terms due to the higher relative content of clays (Fig. 7). Furthermore, in the ternary diagram on the right is possible to see that most loess of Argentina cluster around the C-horizons mean composition, evidencing that the incipient weathering signature of the soils' parent materials resembles that of the loessic sediments (Fig. 7).

Some elemental ratios have also proved to be useful to evaluate the degree of chemical alteration in sediments and soils. For example, the Ba/Sr and Rb/Sr elemental ratios rapidly increase during the initial stages of weathering as a result of the greater alteration rate of plagioclase when compared to K-feldspar (e.g., Nesbitt et al., 1980). Ba/Sr and Rb/Sr ratios in the studied soils are shown in Table 2, and the resulting diagram is displayed in Fig. 8. It is clear that profiles 3 and 2, as well as the A-horizon of profile 1, plot close to the unweathered UCC composition, while profile 4 exhibits a linear trend towards more weathered terms. Fig. 8 also shows the regression lines of these elemental ratios for the bulk samples and fine fractions. It is noticeable that both correlations (i.e., bulk samples and fine fractions) exhibit different slopes, which could indicate that in each group of samples these ratios change at a different rate. However, this change is not gradual but rather random along profile 4 (Fig. 8), suggesting that in this case the Ba/Sr and Rb/Sr elemental ratios are mainly inherited form the parent material which comprises not only loess but also local sources.

3.4. Statistical approach

The preceding geochemical analysis has shown that the chemical imprint of the studied soils seems to be mainly inherited from the parent material (i.e., allochthonous loessic sediments and local alluvial sediments). Thus, weathering and/or pedogenesis do not appear to have substantially modified its chemical signature. To test this assumption, we used statistical tools on a set of geochemical data.

Table 4 shows the Spearman's rank correlation coefficient for major and selected trace element concentrations in the bulk samples of the studied soils. Statistically significant coefficients are indicated in bold. The high correlations between Ti, Zr, Y, Nb, Th and Hf are probably controlled by the presence of heavy minerals such as zircon and rutile. On the other hand, significant associations between Al, Mg, Fe and Mn suggest the occurrence of ferromagnesian minerals (i.e., pyroxenes, amphiboles, biotite). The presence of micas and detrital clay minerals is evidenced by positive correlations of K, Zn, Rb, Ba, Cs, and V, which are elements usually hosted in muscovite, biotite, and illite.

Multivariate cluster analyses for variables (i.e., geochemical parameters) and for cases (i.e., soil horizons) were performed. In both cases the optimal number of groups was two, with an average silhouette width of 0.43 for the geochemical parameters and of 0.33 for the horizons. Fig. 9a shows the cluster analysis dendrogram for selected chemical parameters, where it is possible to distinguish the two groups of elements mentioned above. The first group, composed by the association of Al, Fe, Mn, Mg, Ni, Cs, K, Rb, Zn, Ba, V and REEs (Fig. 9a), which can be found in ferromagnesian minerals and micas, evidences the chemical imprint of the local sources, i.e., metamorphic rocks of the basement and sedimentary rocks of Estancia Belgrano Formation. On the other hand, the second cluster of elements, represented by As, Hf, Zr, Sr, Na, Nb, Th, Ti, Y and U, likely reflects the chemical signature of loess since these elements are hosted in volcanic glass, heavy minerals and feldspars, which have been reported as constituents of the loessic sediments in the Pampean region (e.g., Nicolli et al., 2010). This assumption is reinforced by the similar average silhouette values for both clusters of elements, close to 0.44 and 0.43 for the first and the second group, respectively.

Fig. 9b shows the dendrogram obtained for the soil horizons, where two clusters are also evident. The first group is represented by the horizons of profile 4, whereas the second group includes all horizons of profiles 2, 3, and the A-horizon of profile 1. These associations clearly reveal the geochemical differences above recognized, which can be attributed to the signature of the parent material, also reflected in the textural difference between profile 4 and the other soils of the *catena* (Table 1). These results confirm once again the assumption that the parent material of profile 4 is composed not only by loess but also by alluvial sediments from local sources. Moreover, the average silhouette value for the first group of horizons was 0.24, whereas for the second cluster it was 0.40, thus indicating larger differences between the horizons of profile 4 than among all the other soil horizons.

4. Conclusions

Four soil profiles of a catenary sequence developed under semiarid conditions in the eastern foothills of the Sierra Chica de Córdoba, central Argentina were studied. All studied soils were defined as Mollisols,

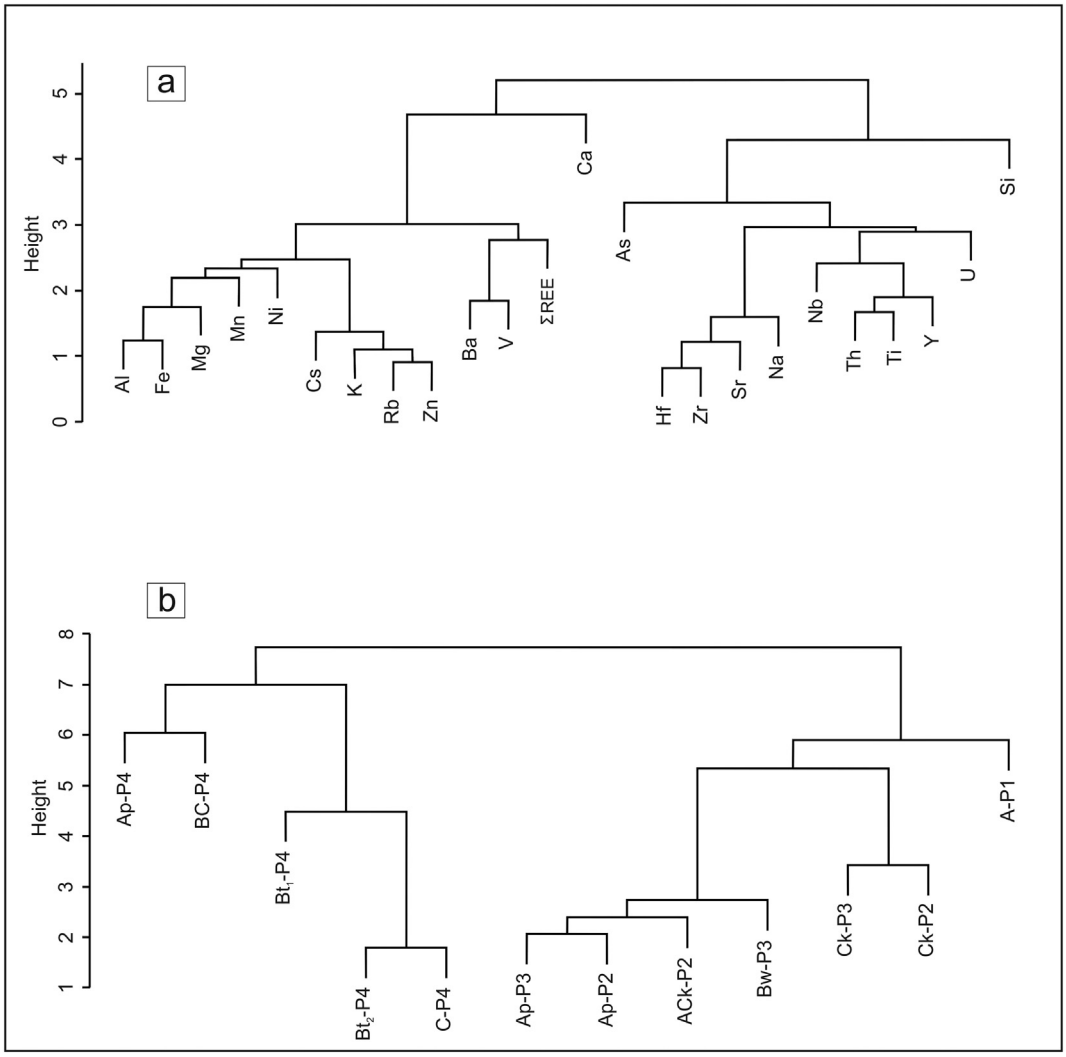

Fig. 9. Dendrograms from hierarchical clustering of geochemical parameters a) and soil horizons b).

classified from the top to the floor of the *catena* as Paralithic Haplustoll, Entic Haplustoll, Udic Haplustoll and Udic Argiustoll.

The pedogenic processes recognized in all profiles are decarbonatation-carbonatation, melanization and argilluviation, which are responsible for the differentiation of genetic horizons along the *catena*. The Udic Arguistoll is more developed because of its catenary position (i.e., in the toeslope), where a higher water infiltration is possible, thus allowing a better differentiation of horizons.

The contents of major, trace and REE in the studied soils are, in general, similar to those of the UCC. Only weak depletions of mobile elements (Ca, Na, Mg, Sr, U) and other elements, such as Fe, Cr, Co and Ni, as well as an enrichment in As can be recognized. The slightly differences detected are due to the chemical nature of the parent material and an incipient chemical alteration. The significant enrichment of As compared to the UCC is inherited from the pampean plains' loess of Argentina. The Haplustolls show little compositional differences between the solum and the parent material, which are only evident through a slightly decrease of Ca, Mg and P. In the Argiustoll, which exhibits a better horizons' development, a larger compositional variation was recorded, particularly in the distribution of REEs. This is mainly a result of the addition of alluvial material in this profile. Weathering indices, such as CIA and ICV, and elemental ratios (Ba/Sr, Rb/Sr) indicate that the soils exhibit an incipient degree of chemical alteration, which is coherent with a weathering-limited denudation regime, such as the one prevailing in the study region. In addition, the A-CN-K ternary diagrams show not only a low degree of weathering but also the chemical imprint of the loess material.

Multivariate statistical cluster analyses have proven to be useful tools to explain the variability between the parent material and solum in the studied *catena*, evidencing that the geochemical signature of the parent material is preserved in these soils.

The studied soils are developed over materials recently deposited, in which the factors of soil formation, such as time, geological history and climatic conditions, have determined a low chemical alteration of primary minerals. Thus, the slight geochemical differences observed along the *catena* are the result of weak weathering and pedogenic processes, which have not been strong enough to mask the chemical imprint of the parent material.

Acknowledgements

This research was funded by Agencia Nacional de Promoción Científica y Tecnológica (ANPCyT, PICT-2012-0275), the Consejo Nacional de Investigaciones Científicas y Técnicas (CONICET, Argentina, PIP 112-200801-03160), and the Universidad Nacional de Córdoba (SeCyT, UNC 05/I711). The data presented here are part of the bachelor thesis of V. Ferreyra. We thank R. Pereira for his assistance in field work and the owners of the Puerta de Fierro farm, where the soils were sampled. We also thank G.A. Sacchi for her assistance in the

profiles description and for her constructive comments. V.A. Campodonico and S. Rouzaut acknowledge a postdoctoral fellowship from CONICET. A. I. Pasquini is member of CICyT, CONICET.

References

Argüello, G.L., Sanabria, J.A., 2003. Aspectos Geomorfológicos y Estratigráficos en la génesis y evolución de la Depresión Periférica. Córdoba. Actas II. Congreso Argentino de Cuaternario y Geomorfología, San Miguel de Tucumán, pp. 177–184.

Argüello, G.L., Dohrmann, R., Mansilla, L., 2012. Capítulo I Loess of Córdoba (Argentine) Central Plain, present state of knowledge and new results of research. In: Rossi, Miranda (Eds.), Educational, Geographical and Cultural Issues, New York, pp. 1–49.

Aubert, D., Stille, P., Probst, A., 2001. REE fractionation during granite weathering and removal by waters and suspended loads: Sr and Nd isotopic evidence. Geochim. Cosmochim. Acta 65 (3), 387–406.

Aubert, D., Stille, P., Probst, A., Gautier-Iafaye, F., Pourcelot, L., Del nero, M., 2002. Characterization and migration of atmospheric REE in soils and surface waters. Geochim. Cosmochim. Acta 66 (19), 3339–3350.

Bini, C., Sartori, G., Wahsha, M., Fontana, S., 2011. Background levels of trace elements and soil geochemistry at regional level in NE Italy. J. Geochem. Explor. 109, 125–133.

Bremner, J.M., Mulvaney, C.S., 1982. Nitrogen total. In: Page, A.L. (Ed.), Methods of soil analysis. Part 2. Chemical and Microbiological Properties. 2nd. Agron. Monog vol. 9. Am. Soc. Agronomy Soil Sci. Soc. Am., Madison, Wisconsin, USA, pp. 595–624.

Buffa, E., Ratto, S., 2009. Contenido pseudototal de cobre, zinc, hierro y manganeso como estimador del fondo geoquímico en suelos de la llanura chaco- pampeana de Córdoba, Argentina. J. Soil Sci. 27 (2), 185–198.

Campodonico, V.A., Martínez, J.O., Verdecchia, S.O., Pasquini, A.I., Depetris, P.J., 2014. Weathering assessment in the Achala Batholith of the Sierra de Comechingones, Córdoba, central Argentina. I: granite regolith fractionation. Catena 123, 121–134.

Candiani, J.C., Stuart-Smith, P., Gaido, F., Carignano, C., Miró, R., Lopez, H., 2001. Hoja Geológica 3163-I. In: María, Jesús (Ed.), Programa Nacional de Cartas Geológicas de la República Argentina 1:250.000. SEGEMAR.

Carson, M.A., Kirkby, M.J., 1972. Hillslope form and process. Science 178, 1083–1084.

Caspari, T., Bäumler, R., Norbu, C., Tshering, K., Baillie, I., 2006. Geochemical investigation of soils developed in different lithologies in Bhutan, eastern Himalayas. Geoderma 136, 436–458.

Chittamart, N., Suddhiprakarn, A., Kheoruenromne, I., Gilkes, R., 2010. The pedogeochemistry of Vertisols under tropical savanna climate. Geoderma 159, 304–316.

Cox, R., Lowe, D.R., Cullers, R.L., 1995. The influence of sediment recycling and basement composition on evolution of mudrock chemistry in the southwestern United States. Geochim. Cosmochim. Acta 59 (14), 2919–2940.

Depetris, P.J., Pasquini, A.I., Lecomte, K.L., 2014. Weathering and the Riverine Denudation of Continents. Springer, Berlin, p. 95.

Döering, A., 1907. La Formation Pampéenne de Córdoba. Revista del Museo de La Plata, pp. 461–465 XIV (Serie 2, 1).

Dorronsoro, C., Aguilar, J., 1988. El proceso de iluviación de arcilla. Anales de Edafología y Agrobiología. XLVII, pp. 310–350.

Elderfield, H.R., Upstill-Goddard, R., Sholkovitz, E.R., 1990. The rare earth elements in rivers, estuaries and coastal sea waters: processes affecting crustal input of elements to the ocean and their significance to the composition of sea water. Geochim. Cosmochim. Acta 54, 971–991.

Frenguelli, J., 1918. Notas preliminares sobre la constitución geológica del subsuelo en la ciudad de Córdoba. Boletín de la Academia Nacional de Ciencias de Córdoba. XXIII, pp. 203–220.

Gallet, S., Jahn, B., Lanoë, B., Dia, A., Rosello, E., 1998. Loess geochemistry and its implications for particle origin and composition of the upper continental crust. Earth Planet. Sci. Lett. 156, 157–172.

Gordillo, C.A., Lencinas, A.N., 1979. Sierras Pampeanas de Córdoba y San Luis. In: Turner, J.C. (Ed.), Segundo Simposio de Geología Regional Argentina. Academia Nacional de Ciencias, Córdoba, pp. 577–650.

Hannigan, R., Sholkovitz, E., 2001. The development of middle rare earth element enrichments in freshwaters: weathering of phosphate minerals. Chem. Geol. 175 (3–4), 495–508.

Heusser, J.C., Claraz, G., 1866. Essai pour servir a une description physiqye et geognostique de la province argentine de buenos ayres. Memoire Societé Helvetique Science Naturelles. vol. 21, p. 139.

Hinton, T.G., Kaplan, D.I., Knox, A.S., Coughlin, D.P., Nascimento, R.V., Watson, S.I., Fletcher, D.E., Koot, B.J., 2006. Use of illite clay for in situ remediation of 137Cs-contaminated water bodies: field demonstration of reduced biological uptake. Environ. Sci. Technol. 40, 4500–4505.

Hofmann, A., 1988. Chemical differentiation of the Earth: the relationship between mantle, continental crust, and oceanic crust. Earth Planet. Sci. Lett. 90 (3), 297–314.

Hu, Z., Haneklaus, S., Sparovek, G., Schnug, E., 2006. Rare earth elements in soils. Commun. Soil Sci. Plant Anal. 37 (9–10), 1381–1420.

Iriondo, M.H., 1997. Models of deposition of loess and loessoids in the Upper Quaternary of South America. J. S. Am. Earth Sci. 10, 71–79.

Jenkins, D.A., Jones, R.G.W., 1980. Trace elements in rock, soil, plant and animal: introduction. In: Davies, B.E. (Ed.), Applied Soil Trace Elements. John Wiley and Son Ltd., pp. 1–20.

Johanesson, K., Zhou, X., 1999. Origin of middle rare earth element enrichments in acid waters of a Canadian High Arctic lake. Geochim. Cosmochim. Acta 63 (1), 153–165.

Kraemer, P., Tauber, A., Schmidt, T., Rame, G., 1993. Análisis cinemático de la falla de Nono. Evidencia de actividad neotectónica. Valle de San Alberto, Pcia. de Córdoba. Actas del XII Congreso Geológico Argentino y II Congreso de Exploración de Hidrocarburos, Mendoza. vol. 3, pp. 277–281.

Laveuf, C., Cornu, S., 2009. A review on the potentiality of Rare Earth Elements to trace pedogenetic processes. Geoderma 154, 1–12.

Levitan, D., Zipper, C., Donovan, P., Schreiber, M., Seal II, R., Engle, M., Chermak, J., Bodnar, R., Johnson, D., Aylor Jr., J., 2015. Statiscal analysis of soil geochemical data to identify pathfinders associated with mineral deposits: an example from Coles Hill uranium deposit, Virginia, USA. J. Geochem. Explor. 154, 238–251.

Marques, R., Prudêncio, M.I., Rocha, F., Cabral Pinto, M., Silva, M.M., Ferreira da Silva, E., 2012. REE and other trace and major elements in the top solis layers of Santiago island, Cape Verde. J. Afr. Earth Sci. 64, 20–33.

McLennan, S.M., 1989. Rare-earth elements in sedimentary rocks. Influence of provenance and sedimentary processes. In: Lipin, B.P., McKay, G.A. (Eds.), Geochemistry and Mineralogy of Rare Earth Elements. Mineralogical Society of America, pp. 169–200.

McLennan, S.M., 1993. Weathering and global denudation. The Journal of Geology. 101, 295–303.

McLennan, S.M., 2001. Relationships between the trace element composition of sedimentary rocks and upper continental crust. Geochem. Geophys. Geosyst. 2 (4). http://dx.doi.org/10.1029/2000GC000109.

McQueen, K.G., 2009. Regolith geochemistry. In: Scott, K.M., Pain, C.F. (Eds.), Regolith Science. Springer-CSIRO Publishing, Dordrecht-Melbourne, pp. 73–104.

Middelburg, J., van der Weijden, C.J., Woittiez, J.R.W., 1988. Chemical processes affecting the mobility of major, minor and trace elements during weathering of granitic rocks. Chem. Geol. 68 (3–4), 253–273.

Nesbitt, H.W., 1979. Mobility and fractionation of rare earth elements during weathering of a granodiorite. Nature 279, 206–210.

Nesbitt, H.W., Young, G.M., 1982. Early Proterozoic climates and plate motions inferred from major element chemistry of lutites. Nature 299 (5885), 715–717.

Nesbitt, H.W., Young, G.M., 1989. Formation and diagenesis of weathering profiles. J. Geol. 97, 129–147.

Nesbitt, H.W., Markovics, G., Price, R.C., 1980. Chemical processes affecting alkalis and alkaline earths during continental weathering. Geochim. Cosmochim. Acta 44 (11), 1659–1666.

Nesbitt, H.W., Young, G.M., McLennan, S.M., Keays, R.R., 1996. Effects of chemical weathering and sorting on the petrogenesis of siliciclastic sediments, with implications for provenance studies. J. Geol. 104, 525–542.

Nicolli, H., Bundschuh, J., Garcia, J., Falcón, C., Jean, J., 2010. Sources and controls for the mobility of arsenic in oxidizing groundwaters from loess-type sediments in arid/semi-arid dry climates - evidence from the Chaco-Pampean plain (Argentina). Water Res. 44, 5589–5604.

Pasquini, A.I., Lecomte, K.L., Piovano, E.L., Depetris, P.J., 2006. Recent rainfall and runoff variability in central Argentina. Quat. Int. 158, 127–139.

Porta-Casanellas, J., López-Acevedo Reguerin, M., Roquero de Laburu, C., 2003. Edafología para la agricultura y el ambiente. Ediciones Mundi-Prensa, Madrid, p. 929.

Prakongkep, N., Suddhiprakarn, A., Kheoruenromne, I., Smirk, M., Gilkes, R., 2008. The geochemistry of Thai paddy soils. Geoderma 144 (1–2), 310–324.

Prudêncio, M.I., Dias, M.I., Ruiz, F., Waerenborgh, J.C., Duplay, J., Marques, R., Franco, D., Ben Ahmed, R., Gouveia, M.A., Abad, M., 2010. Soils in the semi-arid area of the El Melah Lagoon (NE Tunisia). Variability associated with a closing evolution. Catena 80, 9–22.

Pye, K., 1995. The nature, origin and accumulation of loess. Quat. Sci. Rev. 14, 663–667.

Pye, K., Sherwin, W., 1999. Loess. In: Goudie, A.S., Livingstone, I., Stokes, S. (Eds.), Aeolian Environments Sediments and Landforms. Wiley, Chichester, pp. 213–240.

Qiao, Y., Hao, Q., Peng, S., Wang, Y., Li, L., Liu, Z., 2011. Geochemical characteristics of the eolian deposits in southern China, and their implications for provenance and weathering intensity. Palaeogeogr. Palaeoclimatol. Palaeoecol. 308, 513–523.

Rigby, R.A., Stasinopoulos, D.M., 2005. Generalized additive models for location, scale and shape (with discussion). J. R. Stat. Soc.: Ser. C: Appl. Stat. 54, 507–554.

Sacchi, G., Pasquini, A.I., 1999. Factores y procesos de formación de suelos en el Piedemonte oriental de la Sierra Chica, Córdoba, República Argentina. Rev. Pesquisas. Universidade Federal do Río Grande do Sul. Instituto de Geociências vol. 26 (1), 41–48.

Samouëlian, A., Cornu, S., 2008. Modelling the formation and evolution of soils, towards an initial synthesis. Geoderma 145, 401–409.

Santa Cruz, J., 1972. Geología al este de la Sierra Chica (Prov. De Córdoba) entre La Granja y Unquillo con especial referencia a las entidades sedimentarias. Actas 5° Congreso Geológico Argentino, Carlos Paz. vol. 4, pp. 221–234.

Santa Cruz, J., 1978. Aspectos sedimentológicos de las formaciones aflorantes al este de la Sierra Chica, Provincia de Córdoba. Rev. Asoc. Geol. Argent. 3.

Sayago, J.M., 1995. The Argentinian neotropical loess: an overview. Quat. Sci. Rev. 14, 755–766.

Sayago, J.M., Collantes, M., Karlson, A., Sanabria, J., 2001. Genesis and distribution of the Late Pleistocene and Holocene loess of Argentina: a regional aproximation. Quat. Int. 76–77, 247–257.

Schaetzl, R.J., 2013. Catenas and soils. In: Shroder, J.F. (Ed.), Treatise on Geomorphology vol. 4. Academic Press, San Diego, pp. 145–158.

Schlichting, E., Blume, H.P., Stahr, K., 1995. Bodenkundliches Praktikum. Blackwell Wissenschafs-Verlag, Berlín, p. 295.

Schoeneberger, P.J., Wysocki, D.A., Benham, E.C., Broderson, W.D., 2002. Field book for describing and sampling soils, Version 2.0. Natural Resources Conservation Service. National Soil Survey Center, Lincoln, NE . http://www.nrcs.usda.gov/.

Scott, K.M., 2009. Appendix 2: regolith geochemistry of elements. In: Scott, K.M., Pain, C.F. (Eds.), Regolith Science. Springer-CSIRO Publishing, Dordrecht-Melbourne, pp. 434–452.

Smedley, P.L., Nicolli, H.B., Macdonald, D.M.J., Barros, A.J., Tullio, J.O., 2002. Hydrogeochemistry of arsenic and other inorganic constituents in groundwaters from La Pampa, Argentina. Appl. Geochem. 17 (3), 259–284.
Staff, Soil Survey, 2014. Keys to Soil Taxonomy. Twelfth ed. U.S. Department of Agriculture, p. 331.
Stallard, R.F., Edmond, J.M., 1983. Geochemistry of the Amazon: 2. The influence of Geology and weathering environment on the dissolved load. J. Geophys. Res. Oceans 88, 9671–9688.
Taylor, S.R., McLennan, S.M., 1985. The Continental Crust: Its Composition and Evolution. Blackwell, Oxford, p. 312.
Teruggi, M.E., 1957. The nature and origin of argentine loess. J. Sediment. Petrol. 27, 322–332.
Thanachit, S., Suddhiprakarn, A., Kheoruenromne, I., Gilkes, R., 2006. The geochemistry of soils on a *catena* on basalt at Khon Buri, northeast Thailand. Geoderma 135, 81–96.
Tugulan, L.C., Duliu, O.G., Boja, A., Dumitras, D., Zimicovskaia, I., Culicov, O., Frontasyeva, M., 2016. On the geochemistry of the Late Quaternary loess deposits of Dobrogea (Romania). Quat. Int. 399, 100–110.
Walkey, A., Black, M., 1934. An examination of Degtjareff method for determining soil organic matter and a proposed modification of the chromic acid titration method. Soil Sci. 37, 29–38.
Zárate, M., 2003. Loess of southern South America. Quat. Sci. Rev. 22, 1987–2006.